1997

Thickness measurement of curved multilayered polymer structures using the ultrasonic pulse-echo method.

Hong. Shao
University of Windsor

INFORMATION TO USERS

This manuscript has been reproduced from the microfilm master. UMI films the text directly from the original or copy submitted. Thus, some thesis and dissertation copies are in typewriter face, while others may be from any type of computer printer.

The quality of this reproduction is dependent upon the quality of the copy submitted. Broken or indistinct print, colored or poor quality illustrations and photographs, print bleedthrough, substandard margins, and improper alignment can adversely affect reproduction.

In the unlikely event that the author did not send UMI a complete manuscript and there are missing pages, these will be noted. Also, if unauthorized copyright material had to be removed, a note will indicate the deletion.

Oversize materials (e.g., maps, drawings, charts) are reproduced by sectioning the original, beginning at the upper left-hand corner and continuing from left to right in equal sections with small overlaps. Each original is also photographed in one exposure and is included in reduced form at the back of the book.

Photographs included in the original manuscript have been reproduced xerographically in this copy. Higher quality 6" x 9" black and white photographic prints are available for any photographs or illustrations appearing in this copy for an additional charge. Contact UMI directly to order.

UMI

A Bell & Howell Information Company
300 North Zeeb Road, Ann Arbor MI 48106-1346 USA
313/761-4700 800/521-0600

THICKNESS MEASUREMENT OF CURVED MULTILAYERED POLYMER STRUCTURES USING THE ULTRASONIC PULSE-ECHO METHOD

by

Hong Shao

A Thesis
Submitted to the Faculty of Graduate Studies and Research
through the Department of Industrial and Manufacturing
System Engineering
in Partial Fulfillment of the Requirement for
the Degree of Master of Applied Science
at the University of Windsor.

Windsor, Ontario, Canada

1997

I hereby declare that I am the sole author of this thesis. I authorize the University of Windsor to lend this thesis to other institutions or individuals for the purpose of scholarly research.

Hong Shao

I further authorize the University of Windsor to reproduce this thesis by photocopying or by other means, in total or in part, at the request of other institutions or individuals for the purpose of scholarly research.

Hong Shao

The University of Windsor requires the signatures of all persons using or photocopying this thesis. Please sign below, and give an address and the date.

Abstract:

Ultrasonic inspection is accomplished by using electronically controlled pulses introduced into a material from an outer surface. Then, the ultrasonic energy travels within the material, finally reaching again an outer boundary. Material condition is diagnosed from characteristics of the receive ultrasonic energy. The technique of using ultrasonic pulse echo to investigate and examinate the thickness of curved multilayered structures will be presented in this thesis. It also studied physics conditions which the curvatures of multilayered polymer systems might effect thickness measurements. The real location of the focus of an acoustic beam in curved layered structures was calculated by a ray-optical model. Experimental results using the ultrasonic pulse-echo measurement system are presented. The optimization of the focal distance is discussed.

DEDICATION

To My Parents

ACKNOWLEDGMENTS

I would like to express my sincere gratitude to my research supervisor Dr. S.M. Taboun and Dr. R.G. Maev of the University of Windsor. The successful completion of this thesis depended on their useful ideas and constant encouragement. The timely guidance and assistance provide by E. Yu. Maeva, the University of Windsor; Dr. V.M. Levin and Dr. S.A. Titiov, Acoustics Research Center, Moscow, Russia are deeply appreciated.

I would also like to thank Mr. Eric Clausen and Mr. Louis Beauday, department of Physics, and Ms. Jacquie Mummery, secretary of the Industrial and Manufacturing Systems Engineering, for their help and assistance. I would also like to thank Mr. Dave Banninga, Academic Writing Center, University of Windsor, for his assistance and help.

I would like to thank my parents for their love, support and encouragement during the entire period of my education.

Finally, I would thank my wife Sue (Xuewei) Chen, who patiently endured difficult times, and her invaluable support has contributed to the completion of this dissertation.

TABLE OF CONTENT

LIST OF TABLES

Table Page

LIST OF FIGURES

Figure Page

CHAPTER 1

INTRODUCTION

1.1 General

The role of polymeric materials in engineering applications continues to increase throughout industries where metals were historically the major useful choices. The advantages in cost, weight, ease of fabrication and often strength of polymeric base systems are accepted today, and the development of specialized polymers with specific properties is accelerating. A modern automobile contains over 300 pounds (150 Kg) of plastics, and this is not including paints, the rubber in tires, or the fibres in the tires and upholstery. The applications of polymers are already impressive and will become even more in the future.

In the 1940s, adhesive bonding methods became more important in structural bonding when the aircraft industry promoted their use as structural bonding agents. The subject of adhesives became even more interesting to scientists when the application of synthetic resins as adhesives for wood, rubber, glass, metals and plastics was discovered. Adhesives is a technologically important application of polymers. An adhesive has been defined as a

substance capable of holding materials (adherents) together by surface attachment. Adhesives offer a number of significant advantages as a means of bonding: (1) They are often the only practical means available, particularly in the case of small adherents. (2) In the adhesive joining of large adherents, forces are fairly uniformly distributed over large areas of adherent, resulting in low stress, thus lowing the possibility of adhered failure. An adherent layer in a bonded structure can be composed of various types materials which may be different in composition, coefficients of expansion, module, density and thickness. It is also possible to join complex shape, such as curvature, round shape. The adherent layers in a bonded structure provide high cohesive strength, in addition, their excellent creep resistance properties make them ideal for structure application.

However, as with any technology, there are some difficulties in make bonding processes perfect. For instance, during curing of an adhesive layer, the processing temperature, pressure, humidity conditions and different coefficients of thermal expansion of the adherent material and adherents could affect to adherent layer thickness in the components which might cause poor bonding of the structure, especially for layered polymer systems. Therefore, it is necessary to identify the thickness of each adhesive and adherent layer. In the next section, problems regarding the layer thickness are discussed.

1.2 Statement of the problem

The plastic industry produces a variety of large containers for which special safety regulations apply. Among these are canisters and drums for dangerous goods, shock-proof drums, and especially motor-vehicle fuel tanks. A minimum of wall thickness is laid down in all acceptance specifications for these containers. Thus thickness measurement is an important element of the production process and also in quality testing and control.

In our case, an opaque layered plastic composite with a system of internal layers was investigated. A typical composite have five different polymer layers (see, Figure 1.1) high-density polyethylene (HDPE) as a bottom layer; another HDPE with black pigment filler and absorb acoustical energy strongly as a upper layer; Ethylene Vinyl Alcohol Copolymer Resin (EVON) as a barrier layer; and polyethylene based ADMER resin as a glue layers on both sides of barrier EVAL layer. One of the difficulties in the study of this material is very high absorption of most of the layers (Table 1.1)

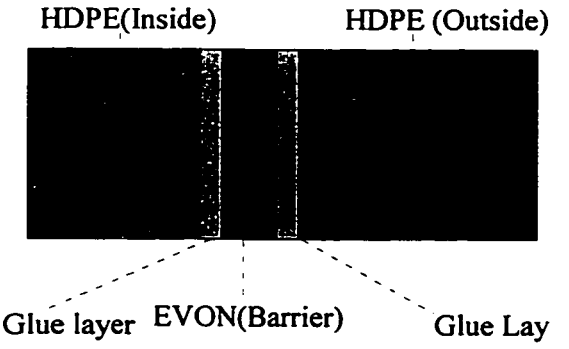

Figure 1. 1 The structure of the experiment sample

Table 1.1 The acoustic properties of the polymer components

Material	HDPE (virgin)	Adhesive ADMER	Barrier EVON	Adhesive ADMER	HDPE (regrind)
%	40	3	4	3	50
[1] Ultrasonic Velocity k m/s	2.36	2.16	3.20	2.16	2.35
[2] Density kg / m^3	0.953	0.92	1.19	0.92	0.953
Impedance $kg / cm^2 s$	224.9	198.7	380.8	198.7	224.0

1. Results from experiments

2. Admer: NF 450A, Standard grade; EVON: Ethylene vinyl alcohol copolymer resin F101; HDPE: Stephen L. Rosin, *Fundamental Principles of Polymeric Materials*, John Wiley & Sons, Inc., pp.45, 1993.

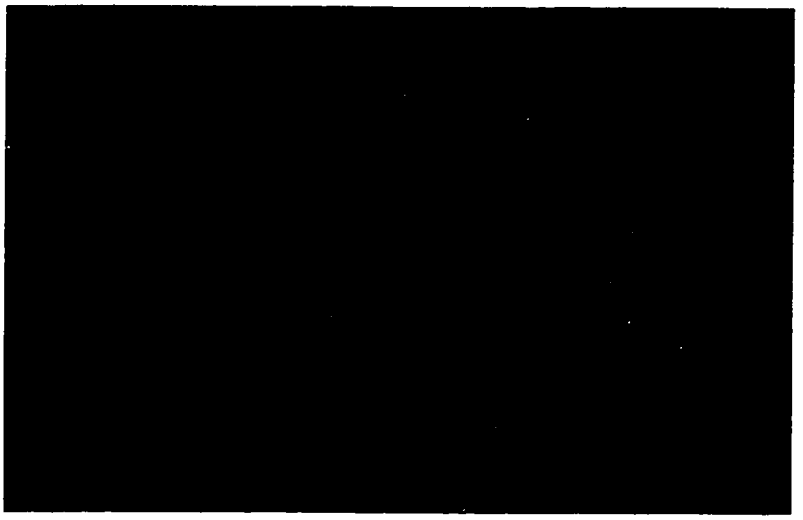

Figure 1.2. Curved Multilayered structure
(B-Scan Obtained by Acoustic Microscopy Imaging Systems B-Scan)

The evaluation of the thickness of thin internal layers of curved structures is a problem that needs to be solved because of the critical protective role played by the barrier layer whose

thickness of adhesive and adherent layers in the bonded component could affect the bonding of the structures.

There are two main difficulties associated with study of this research: One is the curvature of the specimen affected the measurement. The other problem is very high ultrasonic absorption of the most of the layers. In most ultrasonic testing work, geometries are less concerned due to the limited available techniques, most of the measurement were performed in the flat plate geometry. But, practical situations often call for the ultrasonic inspection of objects with curved surfaces [1]. Assessing the acoustic properties of layered structure, based on pulse echo measurements, has been a desirable but difficult goal, as evidenced by the effort over many years in testing material layer characterization. The difficulties in carrying out such characterizations stem from the fact that the received signal is dependent not only on the acoustic properties of the layers, but also on the orientation, shape, surface properties, location and dimensions of the interfaces [2]. The transducer comes into contact with the object at a limited number of points in such cases. Distortion of the ultrasonic beam also will take place if the interface is curved within the ultrasonic beam width. This distorts the geometry of the displayed structure, smears the resolution and in the extreme case can rise to duplicate image artifacts [3]. In the inspection of objects with a curved surface, the acoustic pressure varies with the surface condition changing. These effects can be qualified in terms of the complex spectrum of the receiving electrical signal for a given

transducer. The received ultrasonic signals will be vary and lowering the inspection reliability. When the pulse interact with complicated environments, the pulse spectral decomposition and synthesis is inapplicable because of difficulties associated with the response to each spectral component. Therefore, the interface between the HDPE layer and the adhesive layers is not easy to observe. The problem of the inversion of the ultrasonic data for the thickness of all layers is complicated by the high ultrasonic absorption and weak reflection from the internal boundaries.

1.3 Objectives and Plan of The Research

Research into the use of ultrasonics for nondestructive inspection frequently involves the study of sound with multilayered plate structures. Important research areas include the detection of poor cohesion and adhesive joints, the measurement of the elastic properties and thickness of sheet materials, including carbon fibber composites, polymeric materials, detection the damage of composites, and inspection of surface and layer properties using acoustic emission. Inspection methods for such tasks can be consider broadly use of response methods in which the reflection and transmission characteristics of the plate are examined (e.g., measurement of reflection coefficient), and modal methods which address the plate wave propagation properties of the system (e.g., measurement of Lamb wave velocity). The development of inspection techniques based on either approach requires the study of complicated wave mechanics and relies strongly on the use of predictive modeling

tools to enable the best inspection strategies to be identified and their sensitivities to be evaluated. Based on these feature of ultrasonic techniques, it was considered probable that the ultrasonic technique might provide information on the layer thickness.

The goal of this thesis is to study the application of using ultrasonic pulse-echo method in the frequency range between 10 MHz and 25 MHz for the measurement of the internal layer thickness of a curved multilayered polymer structure. The limitations under specific physical conditions of the measurement is also studied.

The geometry of the problem is depicted in Figure 1.3. An axisymmetric transducer-lens assembly generates an ultrasonic pulse which impinges on a fluid-solid interface. The symmetry axis is assumed oriented per-pedicular to the interface. Upon the reflection, the pulse generates electric pulse in the solid. In the absence of scattering homogeneous, the transducer-lens system will receive the pressure pulse initially reflected from fluid-solid interface, plus and scattering wave signals due to fluid coupling of evanescent modes in the solid, the wave motion in the solid will scatter. A portion of the scattered energy will be transmitted through the fluid-solid interface, and will be received by the transducer.

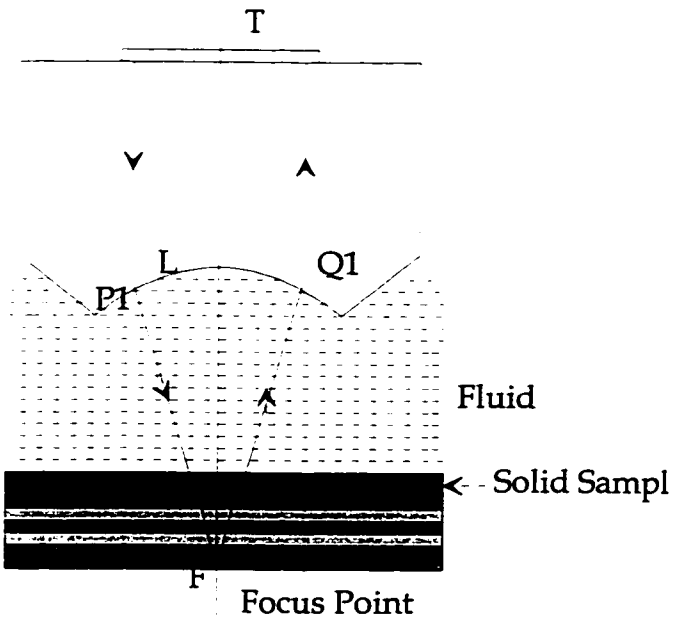

Figure 1.3. Setup of the Ultrasonic Pulse-Echo Experiment

The primary objective of this research is to characterize the physics performance of curved multilayered structure by nondestructive ultrasonic pulse-echo testing technique. In particular, characterization of the curved multilayered structure in terms of the pulse wave reflection, refraction and scattering affected by various geometry and test conditions will be carried out. Due to these conditions, different curvature of the specimen and different physical conditions will be introduced in the test. The effect of each type of these conditions on the mechanical performance of the testing object will be examined and evaluated.

The research is intended to asses the feasibility of utilizing ultrasonic pulse echo techniques in characterization and critical ratio of the curvature of curved structure. On the initial stage, a nondestructive parameter measurable from an ultrasonic pulse echo waveform will

be established. Selection of this pulse echo parameter is based its sensitivity to the geometrical conditions. Factors that affect the measurement of this pulse echo parameter will then be identified and studied. Ultrasonic pulse echo evaluation of the measurement the thickness of curved multilayered polymer structure will be analysis in the time and frequency domains. The prediction of the curvature of the testing objects can be achieved by correlating the pulse echo parameter after the measurement system has been calibrated for geometrical variation of the structures.

Characterization of the multilayered curved structure by non-destructive testing will be carried out in order to verify the results of nondestructive evaluation and determine failure modes with analysis of the critical ratio of the curved surface. The relationship between the failure modes and the geometrical conditions will be determined. It also studied physics conditions which the curvatures of multilayered polymer systems might effect thickness measurements. The real location of the focus of an acoustic beam in curved, layered structure was calculated by a ray-optical model. The optimization of the focal distance was discussed. Numerical simulation was used to predict the optimal distance from lens to the specimen surface from radius curvature and approximately thickness of the specimen. Experimental results using ultrasonic pulse-echo measurement system are presented.

1.4 Formal Presentation

It is the main objective of the present thesis to deal with the nondestructive evaluation of thickness measurement on curved multilayered polymer system. In chapter 2, a briefly review of the basic principles of ultrasonics. Accordingly, chapter 3 of this thesis presents a literature review of nondestructive techniques available today for materials thickness testing. The basic principles of each technique are briefly described. Advantage and limitations in use of these nondestructive techniques are discussed. In present research, nondestructive ultrasonic pulse echo technique is employed to measure the thickness of curved mulitlayered polymer structure. It is therefore considered to be essential for the reader to comprehended the basic principles of this technique and to identify factors that may affect the ultrasonic pulse echo measurement. Hence, chapter 3 is devoted entirely to describe the ultrasonic pulse echo technique. The experiment setup, date collection and analysis will be described and analysis in the rest chapters. Other ultrasonic testing techniques such as Through Transmission Technique, Surface and Lamb Wave Technique and Resonance Method also be mentioned in this chapter.

Chapter 4 deals with the computer-aided ultrasonic pulse-echo system. A computer-based pulse-echo test system and its features were described in this chapter.

In chapter 5, an efficient numerical ray-optical model is described for investigation the ultrasonic beam in a solid material. The numerical simulation of optimal distance from lens to specimen surface is also presented in this chapter.

Chapter 6 will present the ultrasonic pulse echo method to measure and calculate the thickness of each layer of specimen. Results discussion also will presented in this chapter. The experimental work will carry out on both chapter 5 and chapter 6.

Conclusion and future studies are presented in chapter 7.

Chapter 2

PHYSICS OF ULTRASONICS

2.1 Introduction

The ultrasonic technique utilizes high frequency (1-20 MHz) acoustic waves to interrogate the quality of material properties. Ultrasonic waves are simply vibration wave having a frequency higher than the hearing range of the normal human ear, which typically is considered up to be 20,000 cycles per second (Hz). The upper end of the range is not well defined. Frequencies higher than 10^9 Hz, have been generated. However, most practical ultrasonic flaw detection is accomplished with frequencies from 200 KHz to 20 MHz, with 50 MHz used in materials property investigation. Ultrasonic methods have been used widely due to their flexibility and effectiveness in inspecting materials. Different ultrasonic techniques are available for non-destructive inspection of materials properties: (1) Pulse echo (2) Through transmission (3) Interface and plate wave (4) Resonance and (5) Ultrasonic Spectroscope.

2.2 Characteristics of Ultrasonics:

Ultrasonic inspection is accomplished by using electronically controlled pulses introduced into the material from an outer surface. Then, the ultrasonic energy travels within the materials, finally reaching again an outer boundary. Materials conditions are diagnosed from characteristics of the receive ultrasonic energy.

The advantages of ultrasonic testing are that flaws can be detected in metallic and non-metallic materials, flaws distance may be measured from the materials surface, flaws can be located in very thick materials, only single-surface accessibility in required, both internal and surface flaws may be detected, flaw imaging is possible and material properties can be measured. The ultrasonic technique has rapid testing capabilities and portable instrumentation which is available for field testing. Equipment for automatic recording of inspection results is available and the inspection costs are relatively low.

Conversely, there are some disadvantages of the ultrasonic testing. It may be difficulty in coupling energy to rough surface and may be impractical to inspect complex shapes. It is difficult to detect and measure the length of small, tight crack and crack-like discontinuities, when flaw imaging is complex rather than extensive. Training and experience are required

for operators and date evaluators. For special scanning systems, it may be required for inspecting large surfaces.

2.3 Production of Ultrasonic Waves

There are two main ways in which the production of ultrasonic waves may be effected. The first is **magnetostrictions.** It was discovered by Joule in 1847. The phenomenon is frequently employed for underwater sounding , but it is of limited application above the comparatively low frequency of 100,000 cycles per second (100 KC/s). Ultrasonic testing, however, calls for higher frequencies than this, and is therefore based almost entirely on the second method of piezo-electricity.

Piezo-electricity: This method of producing high-frequency oscillation was discovered by J. and P. Curie. Ultrasonic wave propagation requires the presence of a medium such as a fluid or solid. Wave propagation is the vibration or periodic displacement of successive elements of the medium. The low-energy vibrations can travel long distances in many liquid and solid materials. Higher ultrasonic frequencies, however, tend to attenuate rapidly in gases.

The speed of wave propagation, C, usually is expressed in meter (inches) per second, and the excitation frequency f is in Hertz. The wavelength λ is the least distance in the

propagation medium between identical particle displacements, and is given by:

$$\lambda = \frac{C}{f} \qquad ...(2.1)$$

Ultrasonic waves can be generated by any means that agitates liquids and gases or applies small, high-frequency displacements to surface of solid materials. Most methods used to excite ultrasonic energy are electromechanical, such as those making use of piezoelectric crystals and magnetostrictive materials. Other similar methods are electric magnetic and electrostatic. Still other high-frequency generators include whistles, sirens, mechanical vibrators and thermal types such as high-energy laser pulses.

2.4 Ultrasonic Waves

The major types of ultrasonic waves are longitudinal, transverse (shear), and surface. Most of the wave types are named according to relationships to the direction of propagation of the ultrasonic beam.

For longitudinal waves, the propagation and particle motion directions are the same. Since compressional and dilatational forces are involved, they are often called compression or pressure wavea. These waves can propagate in solid, liquid and gases and are the most utilized wave mode for non-destructive testing of materials. Ultrasound cannot travel through gases so easily. Both audible and ultrasonic beams can travel over very long distances through liquids and solids.

Shear wave on the other hand, have particle motion transverse to direction of propagation that is, in a plane perpendicular to the direction of propagation. In some cases the designation SV and SH may be used for shear vertical and shear horizontal. Repetitively, shear wave inspection is generally limited to solid because propagation in liquids occurs only in the very viscous type, while there is no significant propagation of higher ultrasonic frequencies in gases. There are cases where propagation in air is useful in NDE.

Rayleigh or Surface Waves:

There are transverse in character and confined to the surface of solid in which they travel. The peculiar and valuable characteristic of the ultrasonic beam of compression waves which has already been mentioned is that it will travel for very long distances practically unaltered in homogenous liquid or solid matter, but when it reaches a boundary to air, either at a crack or say at back wall of the specimen, it is reflected almost entirely. It is this property which is used to detect and locate the flaw or to measure the thickness of the specimen.

A Rayleigh wave is the one most frequently used in non-destructive testing. These waves an elliptical particle motion in vertical plane and normally travel undispersed on the smooth surface. Surface roughness and sharp curves or currents can cause Rayleigh wave dispersion and reflection. There is no reflection or dispersion of Rayleigh waves around large, smooth corners. Plate waves or Lamb waves are generated when the plate in which waves travel is thin compared with the wavelength. A thin plate can transmit a large number of Lamb wave is a function of plate thickness and ultrasonic frequency.

Lamb wave is type of ultrasonic vibration occurring in plate where the speed is a function of product of the test frequency and part thickness. Wave propagation in plates with frequencies such that the wavelength is comparable to the plate thickness travel in guided mode fashion as Lamb wave (also call plate wave). These waves are highly dispersive, that is, various modes maybe excited, and the speeds vary significantly for slight differences in frequency. Under suitable conditions some modes of Lamb waves can caused to travel with sufficient strength to be useful in non-destructive evaluation of layered materials.

In general, the transducer used to generate ultrasonic wave can be used to detect them. Most ultrasonic instruments operate in the pulse-echo mode, using the same transducer for transmitting and receiving ultrasonic energy. The received pulse will be several times smaller in magnitude than source pulse. The transition from a relatively high energy transmitter to an energy receiver is an accomplished electronically within the instrument. Wave propagation properties are directly related to the elastic properties of the medium and relative size of object. Velocities of the various wave types are determined by modules, density and Poisson's ratio for the particular material in which they are propagation. More specifically, wave velocities can be calculated from the following expression:

Longitudinal wave velocity for bulk materials:

$$C_l = \sqrt{\frac{E(1-\sigma)}{\rho(1+\sigma)(1-2\sigma)}} \qquad ...(2.2)$$

The rod velocity for longitudinal waves (the rod diameter is small compared with a wavelength in the materials):

$$C_l = \sqrt{\frac{E}{\rho}} \qquad ...(2.3)$$

Shear or transverse velocity:

$$C_2 \text{ , } C_t = \sqrt{\frac{G}{\rho}} \qquad ...(2.4)$$

Rayleigh wave velocity for most materials:

$$C_R \approx 0.9 C_t \qquad ...(2.5)$$

where E = Young's modules of elasticity (dynes / cm ^{2})

σ = Poisson 's ratio

C = velocity cm/s

G = modules of rigidity (dynes / cm ^{2})

Echo occurrence at the interface is a function of the acoustic impedance mismatch of the two materials. It defines the acoustic impedance. Impedance calculated from experimental date are given:

$$Z = \rho C \quad gcm^2 s^{-1} \qquad ...(2.6)$$

where ρ = density g / cm ^{3}

C = velocity cm/s

The percentage of incident power that is reflected from boundary between two mediums and how much is transmitted through the boundary when ultrasonic waves are propagation in the media is given by:

$$\frac{Pwr_r}{Pwr_i} = \left(\frac{Z_1 - Z_2}{Z_1 + Z_2}\right)^2 \qquad ...(2.7)$$

$$\frac{Pwr_r}{Pwr_i} = \frac{4 Z_1 Z_2}{(Z_1 + Z_2)^2} \qquad ...(2.8)$$

where Pwr_r = reflected power

Pwr_t = transmitted power

Pwr_i = incident power

Z_1 = acoustic impedance of medium 1

Z_2 = acoustic impedance of medium 2

When a sound wave strikes an interface between two media having different sound speeds, it is bent or refracted in the same manner as light refracts when passing from one material to another having different optical properties. In both cases, for refraction to occur energy must travel at an angle other than normal to the surface. The angle at which sound is refracted is determined by the angle of incidence and velocities of sounding media. In addition to simple refraction of ultrasonic wave at a boundary, mode conversion occurs, which may change the form of wave propagation. A longitudinal wave can be changed into refracted longitudinal and shear waves propagation at different angles, or into a shear wave only.

CHAPTER 3

LITERATURE REVIEW OF THE ULTRASONIC TESTING TECHNIQUES

3.1. Historical Background

The history of ultrasonics is part of the history of acoustics. The earliest record of a scientific examination of music is probably that of Pythagoras, who, in the 6th century BC, discovered that the shorter of two similar stretched strings of unequal length emits a higher note than the longer one and that if one string is twice the length of the other, their pitch differs by one octave. However, records of use of stringed instruments predate Pythagoras by several centuries.

A second notable contribution to the science of acoustics is a published observation by Galileo in 1638 that pitch is associated with vibration. A Franciscan friar named Mersenne, who was a contemporary of Galileo, was the first to actually measure the frequency of a long vibrating string and calculate the frequency of shorter ones from his observations.

A number of physicians and mathematicians laid the groundwork for developing the science of acoustic during the 17th and 18th centuries. Among the familiar names are Robert Hooke (1635-1703), the author of Hooke's law: Joseph Saveur (1635-1716), who first suggested the name acoustics for the science of sound; Brook Taylor (1685-1731), the author of Taylor's theorem on finite series; Isaac Newton (1642-1727), whose law of motion is basic to the wave equations used in ultrasonics; Jean D'Alebert (1717-1783); Joseph Lagrange (1736-1813); and Jean Fourier (1768-1830). The elementary wave equation of D'Alembert and the more elaborate wave equation of Lagrange are basic to an understanding of wave motion. The mathematical series proposed by Fourier, which is a method of expressing an arbitrary function as a series of sine and cosine terms, is ideally suited to the analysis of ultrasonic waves.

Lord Rayleigh published his famous work "The theory of sound" in 1877. This was a milestone in the development of science of acoustics. Rayleigh had worked in his own home with apparatus that was crude according to modern standard, but many of his treaties that resulted from his research are valid today. His work is available in two volumes.

Two 19th century discoveries were significant in the development of methods of generating and detecting ultrasonic energy. The first, magnetostriction, was revealed by Joule in paper published in 1847. Magnetostriction involves a change in the dimensions of a magnetic material under the influence of a magnetic field. The second, piezoelectricity, was

discovered by the Curie brother in 1880. Piezoelectricity is related to the electric charges developed on the surfaces of certain types of crystals when the crystals are subjected detect ultrasonic signals. The inverse effect, in which a voltage impressed across two surfaces of a piezoelectric crystal induces stress in the material, is presently the most common method of generating ultrasonic energy in commercial systems.

Ultrasonics as a specific branch of the science of acoustics had its birth in the study of underwater sound. Prior to the development of ultrasonics as a specific discipline, ships were warned of dangerous obstacles by bells submerged from lightships. Trained crew members of passing ships could detect these warning signals by means of microphones or stethoscopes pressed against the hulls. The invention, in 1912, of the Fressenden oscillator was a decided improvement over the system of bells. The Fressenden oscillator operates electromagnetically at frequencies between 500 and 1000 Hz. It is capable of sending Morse-code messages between ships over distances to 10 miles.

When submarine became a menace to Allies during World War I, Wood and Gerrard in England and Langevin in France were assigned the task of developing methods of detecting enemy vessels. Langevin was the first to suggest using a piezoelectric receiver. Wood made the first directional hydrophone for the location of submarines. Ultrasonics was used in the initial devices to obtain directional beams of energy. Wood and Loomis conducted

some interesting experiments with high-intensity ultrasonics in addition to their studies of the propagation of sound in water.

Since 1940, interest in ultrasonic has increased. Rapid developments in other technologies, such as electronics and piezoelectric ceramics, have made possible the production of practical ultrasonics system for domestic, industrial, and military use. The interesting effects often obtained by the use of ultrasonic energy have sometimes resulted in its being considered as through it were some form of magic. Many impractical uses have been suggested, which reveals that there is a lack of knowledge of the fundamental principles of ultrasonics.

3.2 Ultrasonic Wave Propagation Theory Development

The earliest theory for wave propagation in multilayered media was Lord Rayleigh's deviation in 1885 for waves traveling along the free surface of a semi-infinite elastic half-space. The derivation yields a third order expression whose roots determine the velocity of the propagating surface wave. A generalization of single interface problem was developed by Stoneley in 1924 to describe waves traveling along the interface between two different elastic solids. Later studies addressed the conditions when these waves may travel without leaking into either of the solid and the existence of leaky modes. In 1917 Lamb added

another interface to introduce the notion of a flat layer of finite thickness. His derivation was for plates in vacuum and the roots of his two equations, one for symmetric modes and one for antisymmetric modes, yield the well know Lamb wave dispersion curves. Love showed that transverse modes, involving shearing motion in the plane of the layer, were also possible in layers of finite thickness. Discussions of these and other specific layer geometries may be found in [6-10].

The first derivation of equations for wave propagation in media consisting of arbitrary numbers of flat layers was published by Thomson [11] in 1950. He introduced a transfer matrix which described the displacements and stress at the bottom of layer with respected to those the top of the layers. The matrices for any number of layers could be coupled to yield a single matrix for the complete system. A small error in his derivation was corrected by Haskell [12]. The theory was developed for seismological applications where interest was in surface waves in media consisting of multiple different rock layers. Because the method involves the propagation of the boundary conditions from one boundary of the system to the other via matrix multiplications, it is also referred to as a "propagator matrix" method.

Following Thomson's work, and aided by the availability of digital computers, there was an increase in investigations into the modeling of wave propagation in multilayered media, almost entirely for seismological applications. The models were demanding on the

computer resources which were rather limited at that time and consequently a number of publications, particularly during 1960s, addressed the implementation of the transfer matrix method and the practicalities of solving the response equations or medal equations by computer with maximum efficiency [5, 13].

A development of the theory which received significant attention was the modeling of waves whose amplitude decay with distance along the plate. This was important partly because of the damping properties of the Earth's strata, but mainly because of desire to model leaky wave modes in rock layers. These modes leak energy into adjacent media and their amplitudes thus decay as they propagate. Such solutions were not possible with the original theory and required the introduction of a real exponential factor in the wave equation, achieved by allowing either the frequency or the wave number to be generally complex [5]. A systematic exposition of the theory of the propagation of elastic and electromagnetic waves in layered media was given by L. Brekhovskih [9] in his book "Wave in layer the media". It presented a clear physical picture of the phenomena under his investigation. The simultaneous presentation of the theory of the propagation of elastic and electromagnetic waves, followed in the book, is quite advantageous, since the same mathematical methods may be applied in both cases. The impedance method developed in acoustics have been quite successfully applied in calculation of multilayer reflection reduction of optical system and interference filters.

3.3. Ultrasonic Pulse-Echo Technique

3.3. 1 History and Principles

Pulses echo describes the technique where a pulsed ultrasonic beam is transmitted through a coupling into the material to be tested and travels to another surface of material and then is reflected back to a transducer that may or may not be the transmitting transducer. In this technique, a repetitive ultrasonic pulse is emitted into the tested specimen by a sending transducer and the pertaining echoes are received by the same transducer. Since the emitted inputs compressive wave into the material specimen, pro-propagation and received signals are mostly a composed of longitudinal wave.

Firestone [14] in 1940 was the first to recognize the importance of pulse-echo method for non-destructive testing, particularly for the location of flaws. Earlier, Hiedmann [15] had already used ultrasonic pulse for determining the velocity of sound on the basis of transit time, but in transit-time method, the so-called *sing-around* method. Sokolov [16] in 1941 was the first to publish another intensity-transit time method, the frequency modulation method, for non-destructive testing.

A typical NDE set up pertaining to a Pulse-Echo technique is shown in Fig. 3.1. A single transducer, usually a piezoelectric-type transducer is coupled to the test specimen through suitable coupling medium. The purpose of the coupling medium is to provide adequate wave-transmission through the interface between the transducer and the specimen. An ultrasonic signal is transmitted to the transducer by a signal generator at a particular repetitive rate, which has been provide by a pulse generator. The same pulse triggers a time base generator, which sends the input for the X-axis a cathode rag tub (CRT) display-screen in a digitizing oscilloscope.

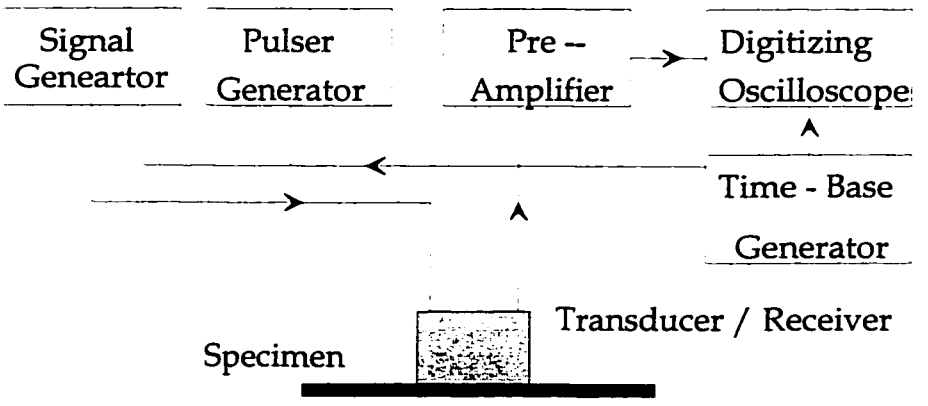

Figure 3.1. Set-up for Ultrasonic Pulse Echo Technique

The reflected portion of the ultrasonic pulse returning back to the transducer is different in voltage. Such variations in voltage are passed to a preamplifier and shown Y-axis of the

CRT. The obtained signal represents the wave reflection from the bottom surface and from any overt flaws in the pathway of the propagation wave.

3.3.2. Construction and Mode of Operation of Pulse-echo Instrument

A typical pulse-echo method for measuring velocity and attenuation equipment arrangement is shown in Figure 3.1. A pulse rf signal of given frequency is converted by means of transducer into a pulsed ultrasonic wave of the same frequency. The ultrasonic pulse travels through the sample and is reflected between the sample boundaries until it decays away. Each time the ultrasonic pulse strikes the sample end coupled to the transducer, an electrical signal is generated which is amplified and displayed on an oscilloscope. If the pulse length is small compared to a round-trip transit time in the sample, a pulse-echo decay pattern develops as shown in Figure 3.1. The velocity of ultrasonic wave propagation is determined by measuring the transit time between the reflected pulse and the corresponding pulse propagation distance in the sample.

A continuously variable time delay may be used to measure the transit time between the pulse that are individually displayed on the oscilloscope by the means of expanded sweep. It is common in such cases to use a detected (i.e., rectified and filtered) signal and to measure the time interval between corresponding reference points of each echo (e.g., the leading edge of the pulse-but see below for refinements). Adjusting the attenuator so that the

receiver input signal is constant for each displayed echo minimizes the error due to amplifier nonlinearisties and reduces (but not eliminate) the uncertainty in the signal reference points. Such a procedure also allows one to read directly the ultrasonic attenuation from the calibrated attenuator.

3.3.3. Literature Review

The technique of ultrasonic pulse-echo measurement material properties, has been adapted broadly recently, especially computer-aided ultrasonic testing opens new possibilities for material diagnostic. In 1985, T. Kundu, A. K. Mal and R. D. Weglein [17] presented the calculation of acoustic material signatures of a multilayered elastic half-space overlain by a fluid. The solid layers are composed of homogeneous isotropic linearly elastic materials and are firmly bonded at interfaces. The calculation procedure is valid at an arbitrarily high frequency of excitation. Results are presented for an uniform single layered and an uniform four layered model for half-space at two frequencies of excitation; one moderate (35 MHz) and other relatively high (370 MHz). They believed that the acoustic material signature is produced by interface between the centrally reflected beam and the beams which are incident on the specimen at Rayleigh angle in their research. The model presented that rays incident on the specimen at other critical angles may also contribute to the acoustic material signature after undergoing

nonspecular reflection. The technique they developed can be useful in predicting the acoustic material signature of a given specimen and in comparing the contribution of the various the various critical refracted waves in specimen.

C. C. H. Guyott and P. Cawley (1987) [18] used pulsed ultrasonic and digital spectral analysis to measurement the through thickness vibration characteristics of plate. The results showed that the use of pulse excitation and digital spectral analysis can give very accurate results, since the testing time required is small, the technique is much more attractive for use in nondestructive testing. In 1992, Chantal Martin, Jean-Jacques Meister, Marcel Arditi and Pierre-Andre Farine [19] presented a novel homomorphic signal processing method for accurate thickness measurement of thin layers from back scattered pulsed ultrasound. It is based on the assumption that the layer is composed of two parallel interfaces. The double-interface signal can be modeled by a pair of Dirace distributions. The ES of the double-interface signal is sinusoidal function in the frequency domain. Its period is inversely proportional to the expected thickness. The logarithmic derivative of the measured signal ES allows for the separation of the contributions which can then be either calculated (straight line in the case of Gaussain envelope signal) or measured by calibration and then removed. After bandpass filtering to eliminate noise, the envelope of inverse Fourier transform is calculated for recovering the periodicity due to the double interface. The main peak of this envelope provides the expected thickness. The method is validated by in vitro experiments at 10 MHz on

Teflon films, where thickness down to 50 μm are recovered, and preliminary in vivid results on arterial wall thickness estimates are presented.

Christopher Graciet and Bernard Hosten (1994) [20] presented a method to measure simultaneously the velocity and the attenuation of ultrasonic waves, the density and the thickness of the sample. Velocity and thickness are deduced from time-of-flight. The Fourier transform of all acquired ultrasonic echoes furnishes the experimental transfer function. Then, they were combined with the expression of plate reflection coefficients to build a form of which the minimum corresponded to the best estimate of density and longitudinal wave attenuation. In their work, the frequency range corresponded to thick plate notions. Wave velocity and sample thickness can be obtained from the measurement of time-of -flight of two successive reflected echoes. As these echoes are separate in time domain, the ratio of their Fourier transforms permits to reach density and attenuation.

3.4. Through Transmission Technique

In the Through Transmission technique, one transducer is emitted the ultrasonic pulses, the other receiving them, they are aligned on opposite sides of specimen. Since the emitter

compressive waves, propagation and received signals are mainly composed of longitudinal Waves.

Figure 3.2 represents an experimental set up for the through transmission technique. This experimental set up may be the same configuration that is used for the pulse echo technique. But with through transmission, two transducers are configuration of this technique as shown in Figure 3.2.

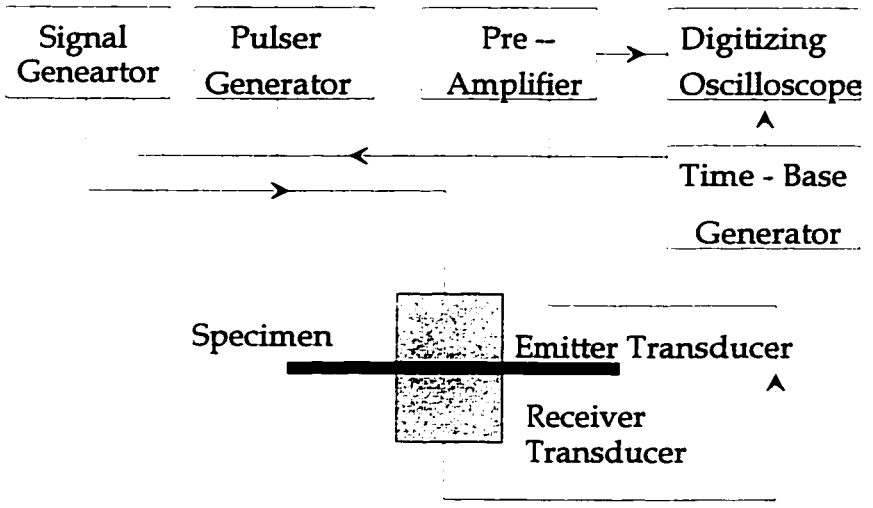

Figure 3.2. Set-up for Ultrasonic Trough Transmission Technique

The main limitation of through transmission technique may be that the ultrasonic wave length is always through thickness of the smallest defected. In addition, some experimental difficulties may be encountered when through transmission technique is applied. Probe

alignment and establishing good coupling (i.e. Between the transducers and the test specimen) on both sides of the specimen could prove to be difficult.

In 1990, M. Bashyam used pulse-echo signals to monitor the thickness of the specimen from through-transmission signals, which provided the actual inspection of the complex-shaped composite structure and generate a C-scan plot independent of thickness [29]. Richard P. Cocker and Richard E. Challis (1993) [21] presented the optimization of the signal processing applied to data generated by a system to measure ultrasound propagation in thin adhesive layers using a short pulse through transmission technique. His method found absorption and velocity as functions of frequency and the real and imaginary parts of the plane waves compressive elastic modules, all measured over a bandwidth of 1 MHz to 60 MHz depending on the adhesive material.

3.5. Surface Wave Techniques

3.5.1 Introduction

Ultrasonic surface waves are separated into different categories, corresponding the two different media: Rayleigh waves, Love waves, Scholte waves, Stoneley waves [28]. Subsequently, we are particularly interested in Rayleigh waves, especially in generalized

Rayleigh wave or leaky Rayleigh wave is made up of combination of two inhomogeneous waves, a longitudinal and transverse wave. Their phase velocities in a direction contained in the interface plane are identical.

3.5.2. Surface Wave Technique Principles

If the incidence of the ultrasonic pulse is purposely at an oblique angle with respect to the specimen surface, Lamb waves resulted. Oblique incidence may be obtained by using edge of θ angle between the emitting transducer and the specimen. Figure 3.3 represents an experimental set up that can be used for the surface and lamb waves techniques. Surface wave propagates on the surface of an elastic isotropic solid without dispersion down to a half-wave length. However, the surface-wave amplitude for a fixed depth diminishes with the increase of input frequency. In practice, surface wave penetration is of the order of the wavelength.

Ultrasonic Lamb waves propagate in a plate or as mode vibration of the plate or tube. They may be understood as complex resonance modes for given frequencies that are functions of the thickness and mechanical properties of the material and of the input-signal wavelength.

In a solid plate with free-boundaries, Lamb Waves result in two groups of symmetrical and antisymmetrical modes. For an increasing ratio of plate thickness to wavelength, the half-amplitudes of the low symmetric, the lowest antisymmetric modes and a surface wave of the same wavelength become very similar. Interference of both Lamb Wave modes gives a quasi-surface wave. Although choosing of an appropriate working point might lead to only one mode, both modes are always present in general testing practice. This explains why both surface and Lamb waves are usually referred a signal method.

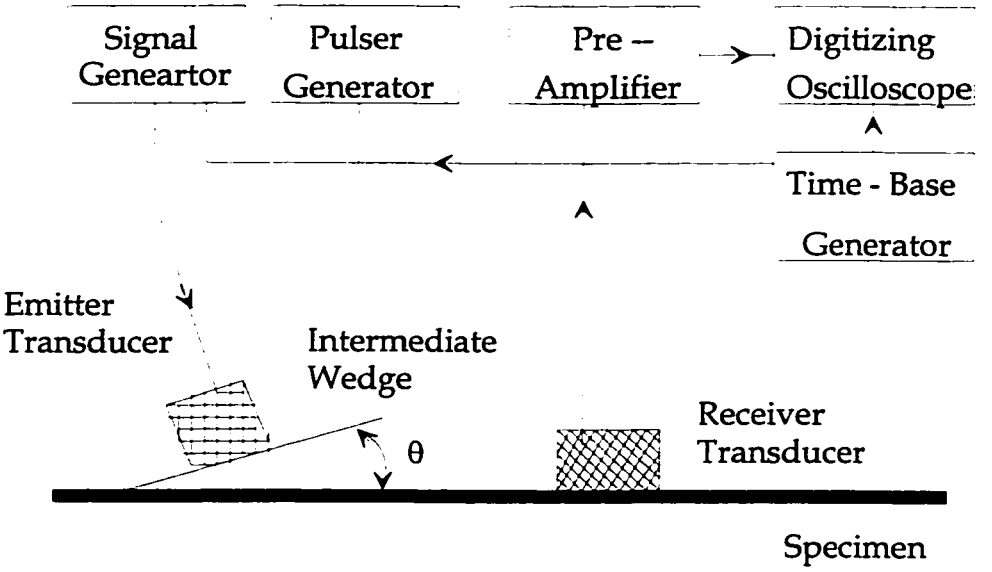

Figure 3.3. Set-up for Ultrasonic Surface Wave Technique

Lamb wave requires a plate or tube of uniform thickness and constant mechanical properties in order to propagation. A change in any of such parameters may cause the wave to be strongly reflected. Dumcumb and Keighley concluded that wave attenuation may either

rise or diminish as a consequence, depending on the overall effect to the resonance phenomenon. Therefore, interactions of propagating surface wave with the inspected specimen can be used in characterizing and quantifying material properties.

3.5.3. Literature Review

Adnan H. Nayfan and Timothy W. Talyor (1987) [22] presented the interaction of ultrasonic waves with multilayerer media. The wave is supposed to be incident from a liquid, at arbitrary angle, upon a plate consisting of an arbitrary number of different material layers. The composite plate is supported from the bottom by solid half-space. It is assumed that all solid interfaces are either rigidly or smoothly bonded. Reflection and transmission coefficients are derived from total system. By examining the behavior of the reflection coefficient, all of the propagation characteristics are identified.

Jens Krause and Bernhard Schwierzi [23] used a mathematical model by Thomson and Haskell [24-26] for description of sound propagation in multilayered structures to calculate the surface acoustic wave velocities for a given system of layers. The evaluation of surface acoustic wave velocities from measured V(z)-curves with high accuracy was performed by means of FFT-algorithm. But, the accuracy of thickness measurements by the method of surface acoustic wave is strongly depended on the composition of layer materials.

Diter Schneider, Thomas Scharwz and Bernd Schultrich (1992) [27] developed to determine simultaneously the thickness and the elastic modules of surface layers from surface wave dispersion. Surface waves with a broad bandwidth are generated by an impulse laser. The pulses are received with inter-digital transducers in the frequency range 12-31 MHz. A Fourier transform technique is used to determine the dispersion curve representing the phase velocity depending on frequency. In the case of normal dispersion in nickel-coated cemented carbide, measurement of dispersion curved in the range up to a ratio of layer thickness to wavelength $d / \lambda = 0.05$, is sufficient do determine thickness and elastic modulus simultaneously. In the case of anomalous dispersion, the surface wave method is less efficient.

3.6 Resonance Methods

The phenomenon of mechanical resonance for some exciting frequencies and its dependence on the specimen dimensions is the principle of NDE-Resonance Methods. In these methods, the frequency of injected ultrasonic wave is varied until specimen resonance is obtained, when such a condition is reached, the so-called resonance standing waves are generated in the materials. At resonance frequency, the wavelength of the standing wave is twice the thickness of the joint given by:

$$\lambda_D = 2\,D = v / f_D \qquad ...(3.1)$$

Where λ_D is the wavelength of standing wave in the joint area; D is the thickness of the joint; v the velocity of sound wave in adherents (the thin adhesive layer is neglected) and f_D is the resonance frequency. As shown in figure 3.4, when there is a void, the resonant frequency will change sharply due to the presence of a gap which is "seen" by the transducer as change of thickness. Therefore the corresponding resonant frequency at new thickness, d is then:

$$d = v / 2f_d \qquad ...(3.2)$$

Resonance-test signals are conventionally carried out for thickness or velocity measurements. Measurements of thickness variation are based on assumption of fixed wave-velocity. Velocity measurements may be based on the obtaining of a resonance condition in a specimen of known thickness.

Resonance methods have traditionally been used for measurement of elastic modules, especially in fundamental studies concerning signal crystal. They were seldom applied to the traditional NDE purpose of material-flaw detection. However, some applications were worked out to address the quantitative testing of material properties by the this technique.

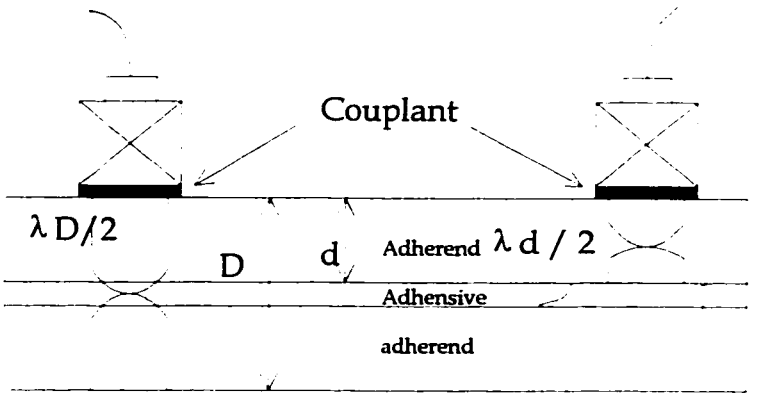

Figure 3.4 . Set-up for NDE Resonance Testing Technique

3.7 Conclusions

Thickness in bonded structures and thin film coating of composite material can be easily measured with the available NDT methods. No single method is universally applicable for measuring the layer thickness of different types materials. Each technique has its own advantages and disadvantages under certain circumstances. The problem of measuring thickness of multilayered curved polymer system is needed to solve in this research. There has been no literature that deals with this problem. This research aims to use ultrasonic pulse-echo method to be effective in determining the layer thickness of curved multilayered polymer systems with acceptable accuracy.

CHAPTER 4

COMPUTER-AIDED ULTRASONIC PULSE-ECHO SYSTEM

4.1 Introduction

The usefulness of ultrasonic waves for the non-destructive evaluation of materials to determine their integrity and uniformity was greatly enhanced by the introduction of the time-domain as a test parameter which led to the pulse-echo test method [30]. Subsequently, at first to improve the spatial resolution of the method, very short pulse was employed [31]. Since such pulses contain a wide spectrum of the frequencies of the incorporation of frequency-domain as a test criterion was a logical further development. The evolving technology which generally is referred to as the ultrasonic spectroscopy has produced not only new insights into ultrasonic evaluation procedures but also complicated the thought process required for the interpretation of test results. It is therefore not surprising that use of frequency-domain in ultrasonic testing that is still mostly confined to the laboratory and has as yet not found its way into the quality assurance shop.

The propose of the development work described here is to simplify the use of the frequency-domain by incorporating it directly into pulse-echo testing without sacrificing the time-domain information.

4.2 Short Pulse Technique

Any pulse can be described both in the time domain and in the frequency domain. In the time domain a signal may be oscillatory. The time domain behaviour is what is seen on an oscilloscope is essentially an instrument for displaying a signal as a function of a time. But varying signal may also be described in terms of the component of each frequency present. This is a frequency domain description and is what is displayed by a spectrum analyzer, just as an optical spectrum indicated the amount of each frequency (or wave length) in a source of light. These two descriptions are related by Fourier transform, which may be written

$$F(f) = \int_{-\infty}^{\infty} f(t) e^{-i2\pi ft} dt \qquad \text{...(4.1)}$$

The convolution of two functions of the same variable, for example G(f) and H(f), can be written:

$$F(f) = \int_{-\infty}^{\infty} G(f') H(f - f') df' \qquad \text{...(4.2)}$$

The convolution operation is a way of describing the product of two overlapping functions. integrated over the whole of their overlap. for given value of their relative displacement.

If a pulse is produced by taking the output of a monochromatic oscillator of amplitude A_o and applying to it a rectangular gate of width t_o. the resulting spectrum will be the convolution of the spectrum of the oscillator (a delta function at f_o) and the spectrum of the gate, giving

$$F(f) = A_0 \cdot t_0 \frac{\sin\{\pi(f - f_0)t_0\}}{\pi(f - f_0)t_0} \qquad ...(4.3)$$

If the pulses are repetitive, with a repetition frequency f_1 then the gated signal is convoluted in the time domain with a comb function. This means that the Fourier transform of signal pulse repetition, which is run a comb function starting at the origin and repeating at intervals of f_1. Thus the frequency spectrum of series of gated pulse is the Fourier transform of the envelope of an individual pulse, centred at frequency of the oscillator, composed not of a continue distribution but of a series of discrete spikes within envelope.

In the ultrasonic pulse echo technique the required signal can be selected not only in the time domain but also in the frequency domain. The problems affect the ability to select the specimen echo and separate it in time from unwanted lens echoes can be the different

parts of acoustic waves from the specimen may be reflected with different time shifts. For example, if the specimen has two closely spaced layers, each of which reflects some energy, or as it often the case, if some of energy is reflected back after coupling into surface waves. If the signal is measured by a peak detector circuit, a reasonable value will be obtained when the interference is constructive. But, when it is destructive, corresponding simply to largest component present, the value will be quit wrong. If very long pulses could be used, they might be possible to measure the middle where the overlap is adequate, but this not practicable when there are constraints on the pulse length, as there are in all high-frequency pulse echoes.

A better approach is to use a narrow-band filter after the gate. This has two effects. First, it improves the signal-to-noise ratio. Second, because of the Fourier relationship, it has effect of smearing out everything in the time domain over a time comparable to twice the length of the pulse. But the filters have a finite bandwidth, causing truncation in time-to-frequency conversion. These truncations give a rise to side-lobes in the reconstructed pulse. It is difficult to be reduced. The other technique that has been used for ultrasonic pulse echo technique is short pulses which is about 1 to 5 of the wave range. The ideal one is one wave range. A schematic circuit is showing in Figure 4.1. A very short impulse is generated by a step recovery diode. The pulse has a width of half the period of the center frequency of the lens; if it is shorter than that the energy in the pulse and it is reduced without any improvement in the signal bandwidth. Thus the lens acts as a sort

matched filter with poor time resolution but an optimal signal-to-noise ratio. The maximum voltage of the pulse, after amplification, is limited to the breakdown voltage of the transducer. The signal passes through a high bandwidth s.p.d.t. switch to the lens, and then back through the s.p.d.t. switch to receiving amplifier. Throughout this part of the system the elimination of electrical reflections is of paramount important. A sampling oscilloscope is used to digitize a signal directly at the frequencies of interest. An analogue voltage generated by the controlling computer determines the time at which a measurement is made of instantaneous value of the signal from the lens, with a time resolution much shorter than the period of the highest frequency present. That value is held for long enough to digitize it at a conventional speed. The measurement delay time is then incremented, and the next point on the waveform is digitized, and so on. In this way the whole waveform can be digitized with a stability of small fraction of a nanosecond. By alternately measuring the signal and with and without energizing the impulse generator, spurious signals due to switching transients can be subtracted out. There may also be small remaining acoustic or electrical reverberations associated with impulse from the generators; these can be subtracted later from recorded waveforms using a reference waveform measured with no specimen present. When such a system is used to observe the reflection from a good reflector at focus point, the signal-to-noise ratio is adequate or direct observation of the trace on the sampling oscilloscope. But in many applications, they require greater accuracy and also greater dynamic range, and then both hardware and software signal averaging can be used.

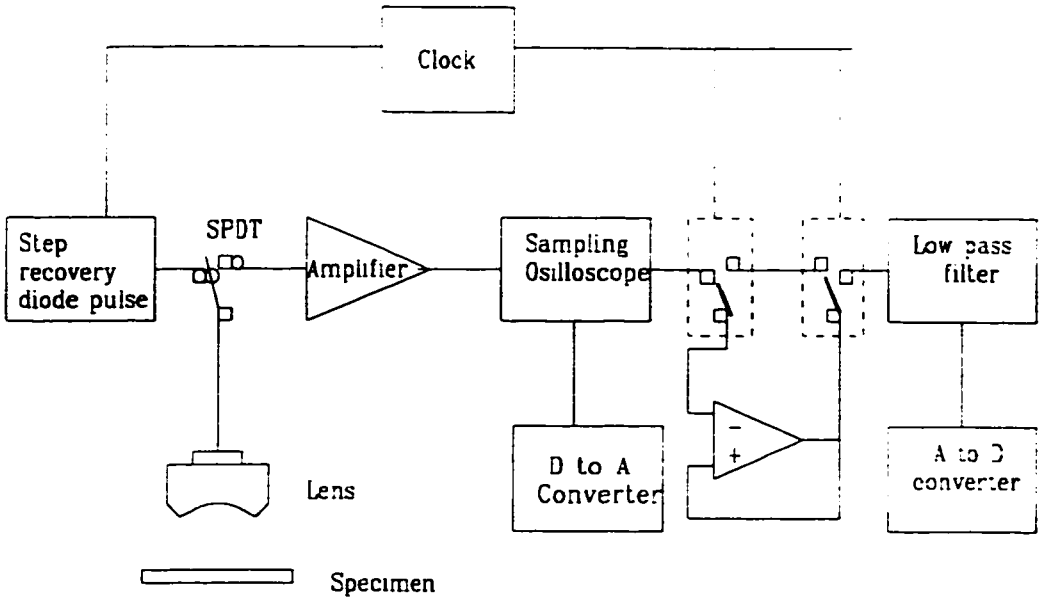

Figure 4.1. Schematic r.f. for very short pulses

4.3 Basic Instrumentation

The basic concept of the approach was derived from earlier work [32] dealing with the investigation of a dual-frequency ultrasonic pulse-echo method. By taking advantage of today computer-aided display technology it was possible to expand the number of frequency ranges used for the test method to three and, at the same time, provide a clear display. Using electronic filters, pulse-echo signals ae extracted from received broad-band echo return and are displayed individually. Although these traces ae shown superimposed on the display, they can therefore clearly be distinguished.

In the following, the computer-aided test system will be referred to as the Multiple-Frequency Pulse-Echo test system to distinguish it from ordinary ultrasonic pulse-echo test equipment.

The components of the test system used for the transmission and reception of broadband pulse-echo signals and for time gating are similar to those used for ultrasonic spectroscopy. In contrast to an ultrasonic spectroscope, however, the received echo-signals are not processed by an electronic or computer-based spectrum analyser. They are instead passed through individually variable filters to select discrete frequency ranges from the broad-band echo return. The analog amplitude versus time functions developed at the outputs of these filters are then digitized and fed into a digital computer equipped with a cathode-ray tube operating system that produces superimposed curves in white. Centre frequency, bandwidth, and output amplitude of electronic filters used the system can be individually adjusted for adaptation to the frequency response characteristic of the ultrasonic transducer and / or the ultrasonic transmission properties of the specimen under test.

4.4 Equipment and Software

The major components of the MFP test system are shown by the schematic block diagram of figure 4.2 and are the following:

Transduce

Pulser/Receiver

Filter-Digitizer, containing:

Time-Gate

Filters

Digitizer

Oscilloscope

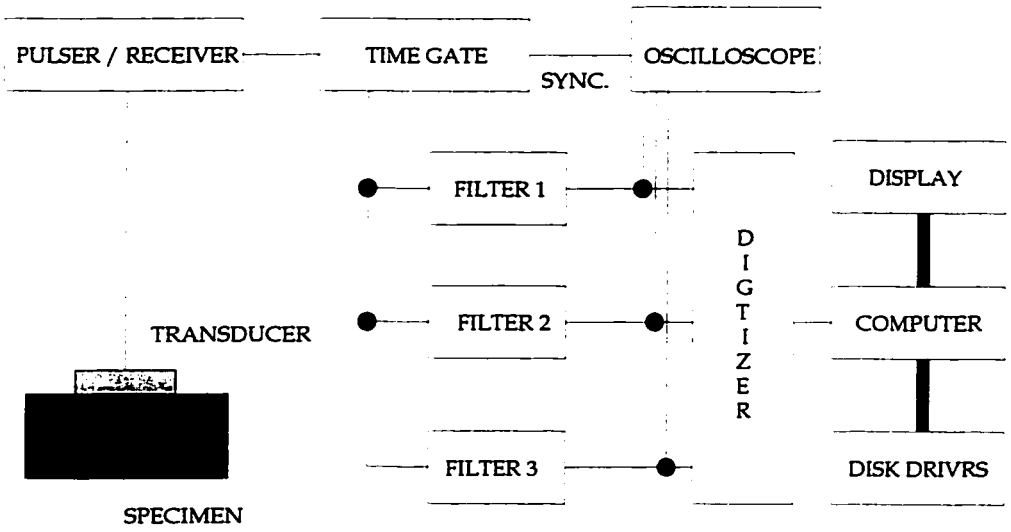

Figure 4.2 Block diagram of pulse-echo test system.

The transducer contains a highly damped piezoelectric element and exhibits therefore a broad response characteristic covering frequencies of up to 20 MHz. The Pulser / Receiver provide the initial pulse excitation of the transducer and amplifies the echo signals the

transducer subsequently picks up from the test specimen. The receiver bandwidth exceeds that of the transducer.

The amplified signals are fed into specially designed equipment called Filter-Digitizer which has several functions. It provides a time gate which is open after an adjustable delay from the onset of the initial pulse and has a duration variable delay from 1 to 50 microseconds. It extracts three ranges of frequencies are from the gate-out signal with the help of filters whose centre frequencies are adjustable within the following, overlapping ranges: 0.75 to 10.00 MHz. The bandwidth of these filters can in addition be individually varied from 0.12 to 1.50 MHz. Their analog amplitude outputs are monitored by an oscilloscope equipped with input channels and trace intensification to render the position of the time-gate visible.

Finally, a digitizer is provided which sequentially converts the three rectified filter output voltages into digital form and sends that date to the computer via a serial port .

For the date transfer, a special; code is used which produces words consisting of two 8-bit date bytes for each point of the time axis. In addition to the amplitude values representing the settings of the Filter-Digitizer, i.e. the delay between the onset of the initial pulse and opening of the time gate, the filter number, its centre frequency and bandwidth. The digitization is carried out over 448 equidistant points on the time axis for each of filter

outputs in turn with a sampling time for a set of date is therefore about 1.4 second. The date received by the computer is processed with help of special software and shown as a display produced by cathode-ray-tube operation system which is part of the computer.

For processing of test date, the SR -9000 Pulser / Receiver Card (Provided by Matec Instruments Inc. 1994) are used employing the testing work. The basic operation has been verified under the DS100 program, which was provided by Sonix. The software package encompassed the following features:

1) The standard 8 voltage ranges are represented. To change voltage ranges, go to the center control display and click on the desired input range. Note that all voltages are displayed as a peak to peak amplitude.

2) The voltage range can be calibrated by changing the vernier gain and voltage offset controls, which are located to the immediate left and right of the voltage input level selector. On both dials, zero (0) represents the factory calibration.

3) The signal type selector (located above the voltage level) can be set at RF (standard bipolar), Video, Logamp, or User. The 31.5 mV and 62.5 mV input ranges are not available in Logamp mode.

4) The video filter setting (located to the right of the signal type selector) is only available when the signal type is set to Video.

5) The sampling rate can be changed from 0.78125 MHz to 800 MHz. The ETS notation to the right of the higher sampling rates denotes 'Equivalent Time Sampling' which involves taking multiple triggers in order to achieve sampling rates above 100 MHz.

6) 'Trigger source' can be set to one of three modes; internal, channel threshold, or digital. The input polarity (trigger on the rising / falling edge of the input waveform) control is located directly below the 'trigger source' input. The 'input polarity' parameter has no effect in internal trigger mode. The threshold level, which is only available in Channel A Threshold mode can be adjusted on the slide scale to the left of the scope display.

7) The 'Sensitivity' selection, which is located directly below the trigger source display, controls whether external triggers occur on edge transitions or on pure amplitude (level).

8) The 'Horizontal offset' control allows scrolling through the waveform. If you are in an external trigger mode and 'post trigger delay' is set to 0, the horizontal offset can be made negative, thus allowing pre-trigger mode.

9) The 'Data collection length' parameter controls how much data is collected after the trigger. This parameter may differ from the number of points specified by the horizontal scope scale.

10) The 'Post trigger delay' parameter controls the number of samples to be ignored after the trigger comes. This control is unavailable in pre-trigger mode.

11) The 'Is recording' light will be lit once for each successful trigger.

12) The 'Num to save' control sets the number of waveforms that will be saved once the 'Start saving' button is clicked. When you click on 'Start saving,' you will be prompted to

enter a filename: the extension is always forced to 'WAVE' The file that is created is an ASCII file, containing all the points of each waveform horizontally, with the waveforms themselves stacked vertically: a0 a1 a2 a3 a4 .... an; b0 b1 b2 b3 b4 .... bn; c0 c1 c2 c3 c4 .... cn, where 'n' is the amount set by 'Data collection length'. This file should be readable by any math package or spreadsheet program, thus allowing post-processing of the data.

CHAPTER 5

RAY-OPTICAL MODEL OF FOCUSED ACOUSTIC BEAM IN REFLECTION ULTRASONIC SIGNAL IN CURVED STRUCTURE

5.1 Introduction of Focused Lens and Focused Acoustic Beam

Several techniques are currently availiable for the non-destructive evaluation of surface related properties of solid material. One of the newest technique is focused-beam, reflection mode for ultrasonic pulse-echo method [33]. The existing experimental evidence shows that many feathers of the focused beam are clearly understood at the present time. Such an understanding can be extremely helpful in developing a rapid, quantitative technique for measuring and monitoring material properties of solids used in many modern, high performance structures and systems.

Focus lens has excellent focusing properties on its axis [34]. The lens basically consists of a disc of sapphire with the axis of the disc aligned accurately parallel to the crystallographic c-axis of the sapphire. In the center of one face of the disc a concave spherical surface is

ground. This surface provides the focusing action and, to optimize transmission, it is coated with a quarter-wavelength thick matching layer. On the other face a thin film of gold is deposited to form a ground electrode. A transducer is then placed on this face, usually by epitaxially growing zinc oxide (ZnO) using vacuum sputtering. Finally, a small dot of gold is deposited an active area of the transducer that is accurately opposite the focusing surface. When the transducer is energized, plane acoustic waves are generated with travel through the disc. In use, the lens is placed in contact with a coupling fluid (usually water), and when the wave cross the spherical interface between the lens and fluid they are refracted towards a focus on axis of the lens. The very high refractive index encountered when acoustic waves pass from a solid to liquid enables the waves to be brought to a good focus with a single lens surface in this way, even when the numerical aperture, and server geomtrical aberrations.

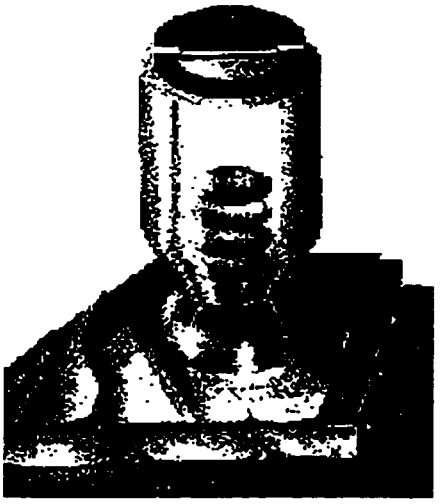

Figure 5.1. Focused Lens

In our experiments, the focusing lenses give more precise measurement than any other type such as flat contact lens and using Gausian beams. The focusing lens produces a convergent beam focused on the particular area to be tested. They concentrated on the small area, and more reflected signals from the material interfaces are received by the transducer / receiver. By contrast, flat contact lens and Gaussian beam contact specimen on a wide area. Only part of the reflected signal comes back to the transducer/receiver. This is the advantage for applying focusing lenses to measure curved solid.

5.2 The Ray - Optical Model

The goal of the present model is to accurately and efficiently predict the response of physically realizable ultrasonic transducer used to inspect curved multilayered polymer system from its interior layers.

The general setup of ray model in the case of focused acoustical system is sketched in Figure 5.2. The transducer T mounted on a solid curved surface generated the pulse wave which propagate normal to the sample surface. Spherical cavity L is severed to focus the incident pulse into a focused convergent beam of acoustic wave in coupling fluid. The acoustic beam is reflected from the solid specimen placed at a distance a from the focus point P of the spheral focus lens. F is the original focus point in the water, P is the new real focus point in the sample. f is the focal distance of the lens. A short pulse with centre

frequency ω is used as input and time gating in the recording device separates the reflected signal from other spurious reflections. Assume the incident ray at point Q. θ is the angle of incident ray and axis. The radius of curvature of the sample is R, with the center at point O. m is the distance from the center of the curvature to the geometrical focused point. l is the distance from the sample surface to real focus point.

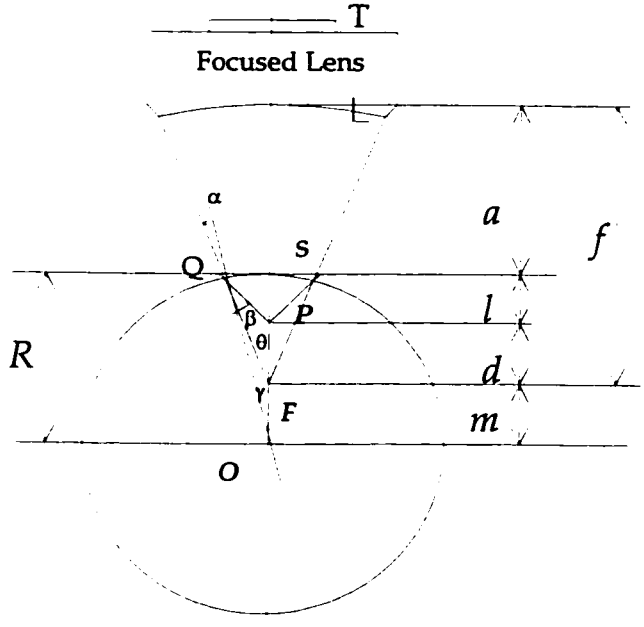

Fig. 5.2. The Ray -Optical Model of Focused Lens with Curved Structure

From figure 5.2:

$$a + l + d = f, \qquad ...(5.1)$$

where b is the distance from the surface of the sample to the lens geometric focused point F.

$$R - l - d = m \qquad ...(5.2)$$

so, we have:

$$m = R + a - f. \qquad \text{...(5.3)}$$

The incident ray at point Q on the sample surface. We assumed the incident angle is α, and the reflected angle is β. By Snell's law:

$$\frac{\sin\alpha}{\sin\beta} = \frac{C_w}{C_S} \qquad \text{...(5.4)}$$

where:

C_W is the ultrasonic velocity in the fluid (water).

C_S is the ultrasonic velocity in the solid.

In the triangle ΔQOF:

$$\frac{R}{\sin(\pi - \theta)} = \frac{|OF|}{\sin\alpha} = \frac{m}{\sin\alpha} \qquad \text{...(5.5)}$$

$$\sin\alpha = \frac{m}{R}\sin\theta \qquad \text{...(5.6)}$$

Substituted equation (5.6) to equation (5.4):

$$\sin\beta = \frac{C_S}{C_W}\sin\alpha = \frac{C_S}{C_W}\frac{m}{R}\sin\theta\,. \qquad \text{...(5.7)}$$

In triangle ΔOQP:

$$\frac{\sin\beta}{\sin\gamma} = \frac{|OP|}{|QP|} = \frac{m+d}{|QP|} \qquad \text{...(5.8)}$$

$$\sin\gamma = \sin(\theta - \alpha). \qquad ...(5.9)$$

In triangle ΔQPF:

$$\frac{|PF|}{\sin(\beta - \alpha)} = \frac{|QP|}{\sin\theta} \qquad ...(5.10)$$

multiply equation (5.8) and equation (5.10), we have:

$$\frac{m+d}{\sin\beta}\sin\gamma = \frac{\sin\theta}{\sin(\beta - \alpha)}|PF| \qquad ...(5.11)$$

$$\frac{m+d}{d} = \frac{\sin\theta\ \sin\beta}{\sin\gamma\ \sin(\beta - \alpha)} = \frac{\sin\theta\ \sin\beta}{\sin(\theta - \alpha)\sin(\beta - \alpha)}. \qquad ...(5.12)$$

Since:

$$\sin\alpha = \frac{m}{R}\sin\theta \qquad ...(5.13)$$

$$\cos\alpha = \sqrt{1 - \left(\frac{m}{R}\sin\theta\right)^2} \qquad ...(5.14)$$

We assumed:

$$p = \frac{m}{R}\sin\theta \qquad ...(5.15)$$

so, we have:

$$p = \sin\alpha \qquad ...(5.16)$$

$$\cos\alpha = \sqrt{1 - p^2} \qquad ...(5.17)$$

where:

$$k = \frac{C_S}{C_W} \qquad ...(5.18)$$

$$\sin\beta = k \cdot p, \qquad ...(5.19)$$

$$\cos\beta = \sqrt{1 - k^2 \cdot p^2}\,. \qquad ...(5.20)$$

insert equations (5.13), (5.14), (5.15), (5.16), (5.17), and (5.18) into equation (5.12):

we will have:

$$\frac{m+d}{d} = \frac{k \cdot p \cdot \sin\theta}{\left(k \cdot p\sqrt{1-p^2} - p\sqrt{1-k^2 \cdot p^2}\right) \cdot \left(\sin\theta\sqrt{1-p^2} - p \cdot \cos\theta\right.} \qquad ...(5.21)$$

if let:

$$q = (k \cdot p\sqrt{1-p^2} - p\sqrt{1-k^2 \cdot p^2}) \cdot (\sin\theta\sqrt{1-p^2} - p \cdot \cos\theta) \qquad ...(5.22)$$

so:

$$\frac{m}{d} + 1 = \frac{k \cdot p \cdot \sin\theta}{q} \qquad ...(5.23)$$

$$d = \frac{m \cdot q}{k \cdot p \cdot \sin\theta - q}\,. \qquad ...(5.24)$$

because:

$$f = a + l + d \qquad ...(5.25)$$

so, we have:

$$l = f - a - d, \qquad ...(5.26)$$

then:

$$l = f - a - \frac{m \cdot q}{k \cdot p \cdot \sin\theta - q} . \qquad ...(5.27)$$

Using equation (5.27) we can calculate the distance from the sample surface to real focused point l, the distance from the lens to the specimen surface a, the lens focal length f, the angle θ and the radius of the curvature of specimen R. Figure 5.3 shows that the distance from lens surface to real focal point is approximately constant for radii of curvature of the specimen greater than 20 mm.

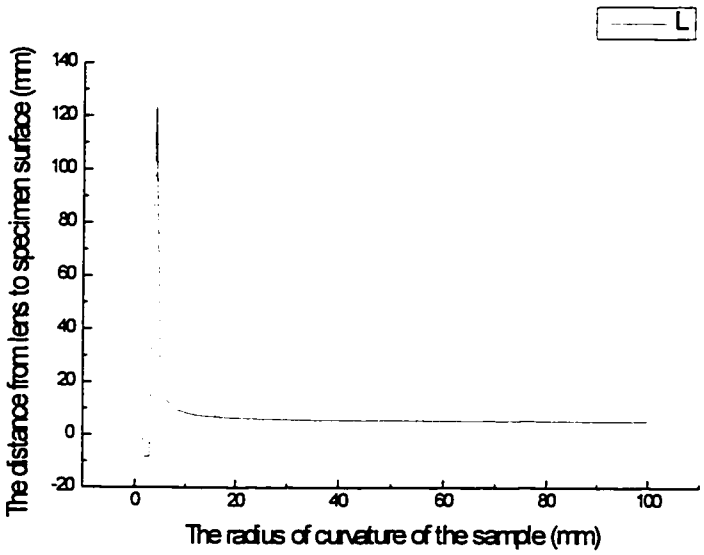

Figure 5.3 The relation between the distance from lens surface to real focus point and the radius of the specimen curvature.

Becaue the distance from the specimen surface to focused to lense is a linear function with the curvature of specimen. We substituted equations (5.12) and (5.22) into equation (5.24):

$$d = \frac{m(k \cdot \sin\theta\,(1-p^2) - k \cdot p\cos\theta\sqrt{1-p^2} - \sin\theta\sqrt{(1-p^2)(1-k^2\cdot p^2)} + p\cos\sqrt{1-k^2\cdot p^2})}{k\cdot p^2\sin\theta + k\cdot p\cos\theta\sqrt{1-p^2} + \sin\theta\sqrt{(1-p^2)(1-k^2\cdot p^2)} - p\cos\sqrt{1-k^2\cdot p^2}}$$

...(5.28)

Let reconsider equation (5.15), and use equation (5.3) instead *m*:

$$p = \sin\theta - \frac{f-a}{R}\sin\theta\,. \qquad \text{...(5.28)}$$

In our case, the angle θ which is the aperture of the lens is $\theta \le 15^\circ$ (for 20 MHz). The most common radius curvature is between the 40 mm to 50 mm. The focal lengths for two lenses used are 19.00 mm for 20 MHz and 12.36 mm for 15 MHz. Usually the radius of curvature, *R* is greater than the lens focal length, *f*. The distance from the lens to specimen surface, *a*, is adjusted to get the best received ultrasonic pulse. In this case $0 < a < f$, so, approximately $p << 1$. Since $k = Cs/Cw \approx 1.5$, so $k^2\cdot p^2 << 1$. On the other hand since angle θ is very small , $\cos\theta \to 1$, then $p\cdot\cos\theta \to p$. Then we look up equation 8: when $p << 1$, $1 - p^2 \to 1$; $1 - k^2\cdot p^2 \to 1$, $p\cdot\cos\theta$ is negligible. Then, the equation 28 will likely be :

$$d = \frac{m\cdot(k-1)}{k+1} = \frac{R\cdot(k-1) - (f-a)\cdot(k-1)}{k+1}\,. \qquad \text{...(5.29)}$$

Then, we substitute equation (5.29) into equation (5.27), to yield:

$$l = (f-a)(1+\frac{1}{k+1}) - (\frac{k-1}{k+1})R, \qquad \text{...(5.30)}$$

$$\text{let}: \quad U = (f-a)\left(1+\frac{1}{k+1}\right) \qquad \text{...(5.31)}$$

$$= \frac{k-1}{k+1} \qquad \text{...(5.32)}$$

$$\text{so}: \quad l = U - V \cdot R. \qquad \text{...(5.33)}$$

Equation (5.33) is a typical line function $l = f(R)$. It means that the distance from the real focal point to a specimen surface is a line function of the radius of the curvature of the specimen. From equation (5.33), we have:

$$a = f - \frac{l + \frac{k-1}{k+1} R}{1 + \frac{1}{k+1}}, \qquad \text{...(5.34)}$$

Where a is the distance from lens to the specimen surface
l is the real focal distance
R is the radius of curvature of the specimen
$k = C_s \ / \ C_w$

5.3 Simulation

The equation (5.34) is used for numerical simulation. We take into account that variation of acoustic velocities in each layer is less then 10% (except barrier layer with higher velocity, but its volume fraction is only about 3%). The ultrasonic velocity in the solid is taken to be the average velocity of the four different materials in the tested sample. The

optimum distance from the lens to the surface only depends on the radius of curvature of the sample. We numerically predicted the optimal distance from the lens to specimen surface from the radius curvature and the approximate thickness of the specimen. The results are shown in Figure 5.4.

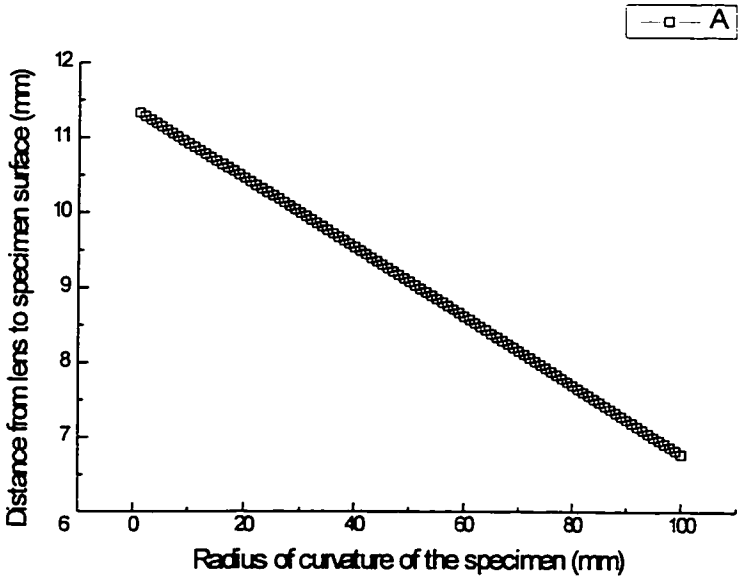

Figure 5.4. The optimal distance from lens to specimen suface.

We conducted a set of experiments to examine our theoretical calculations. For instance, when we have a specimen,which total thickness is 4.50 mm, and its radius curvature is 60 mm, from the above Figure 5.4 we find that the optimum lens distance to sample is 8.61 mm for a 15 MHz focused lens. The signal recorded from oscilloscope is shown in Figure 5.5.

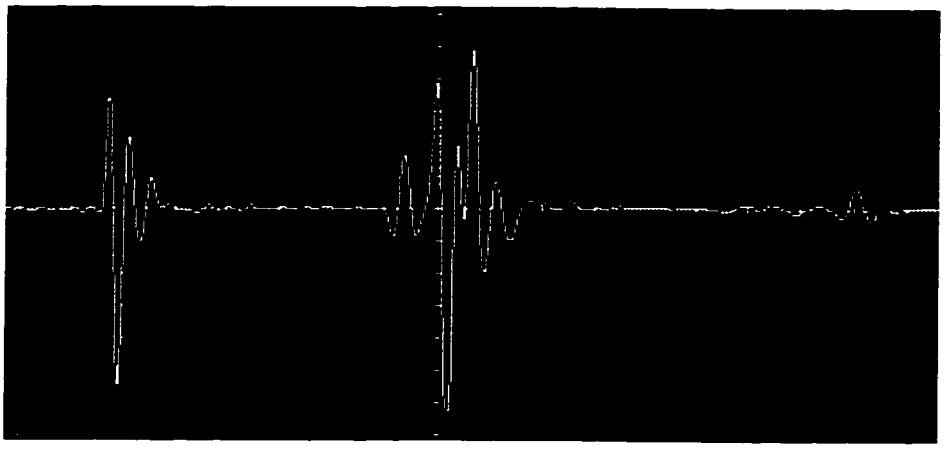

Figure 5.5 Ultrsaonic Signal Recorded from Oscilloscope.
(Curvature: 60 mm, Frequency 15 MHz, Distance from lens to sample surface: 8.61 mm)

In Figure 5.5 at the distance of 8.61 mm from lens to specimen surface, the signals reflected from the interfaces between each of the layers are clear and strong because the real focus point is on the right spot of the sample. When the distance from lens to specimen surface is increased, the results are different.

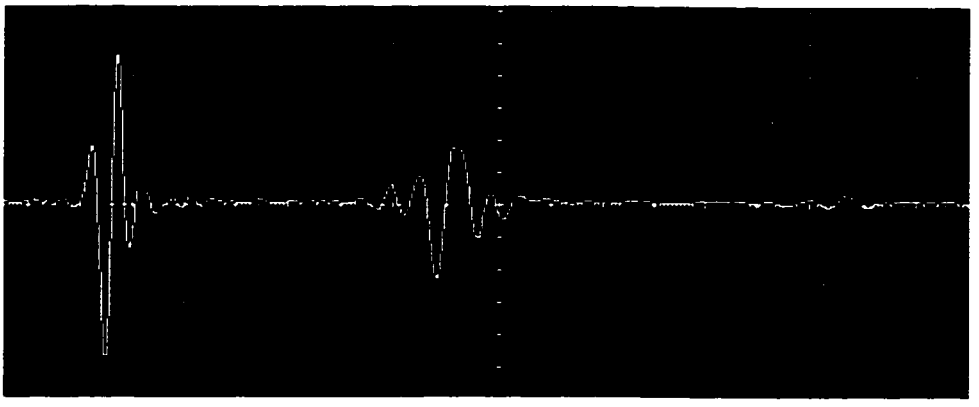

Figure 5.6 The lens far from the specimen.
(Curvature: 60 mm, Frquency 15 Mhz, Distance from lens to sample surface: 12 mm)

In Figure 5.6, the distance from the lens to the sample surface is 12.00 mm. The signals reflected from the barrier layer and the bottom layer are weak because the focus point is near the between water-sample top interface. Because of this less ultrasonic energy reaches the barrier layer, and as a result - the reflected pulse echo signals from the barrier layer and from the HDPE / water interface are very weak.

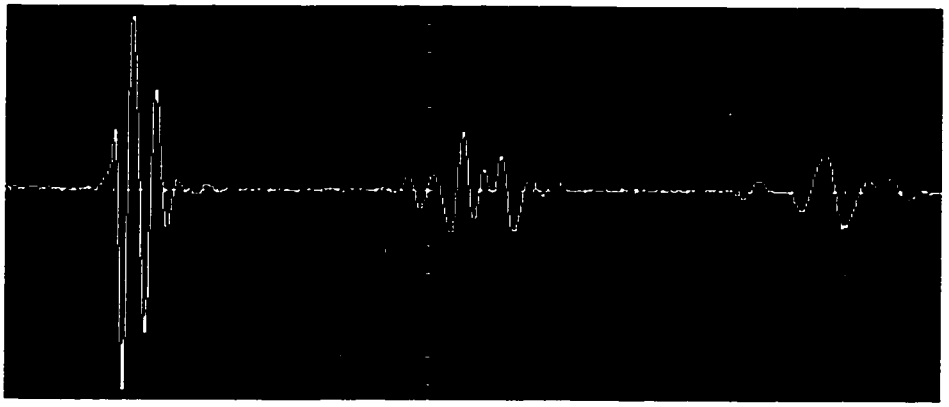

Figure 5.7 The lens is too close to speciman.
(Curvature: 60 mm, Frquency 15 Mhz, Distance from lens to sample surface: 4 mm)

If the lens is too close to specimen, (in our case it's the distance from lens to sample surface is 4.00 mm, the signal reflected from the various layers is not clear and the result is also poor (Figure 5.7)). It is also difficult to determine from this figure which peak is the reflected echo from the interface between the glue and barrier layers. When the lens is too close to the sample, the lens focus is on the far side of the specimen and the oscillogram at the Figure 5.7 shows a strong and clear pulse-echo signal reflected from the interface

between HDPE bottom and the water; but the signals reflected from glue layer and barrier layer are weak. This lens-sample distance is suitable for measurement of the total material thickness, but not for investigation the interior structure details. Satisfactory experiment results can be obtained only at the optimum distance between the lens and the specimen surface.

So, when we inspect a multilayered curved structure we can always apply for equation 34 to approximately adjust the real focus point to the depth to be inspected and have strong, clear reflections.

CHAPTER 6

Ultrasonic Pulse Echo Method Measure Multilayered Structure Thickness

6.1. Introduction

The goal of this study is to investigate the limits of the ultrasonic pulse-echo method in the frequency range between 10 MHz and 25 MHz for the measurement of the internal layer thickness in a curved multilayered polymer structure. We will present the ultrasonic pulse-echo method to measure the thickness of multilayered curved structure. In this test, the thickness of the specimen can be obtained from measurement of a time-delay of two successive reflected echoes which are separate in the time domain. As already mentioned in chapter 5, the optimization technique and the results from numerical simulation will provide the optimal distance between the lens to specimen surface. In our experiments, the focusing lens gave more precise measurements than any other type such as flat contact lens and using Gaussian beams. The focusing lens produces a convergent beam focused on the particular area to be tested. It is more concentrated on the small area, and more reflected signal from the material interfaces is received by transducer/receiver. For processing of test data, the SR-9000 Pulser/Receiver Card

(Matec Instrument, Inc., 1994) was used the testing work. The basic operation has been verified under the DS100 program, provided by Sonics Inc. The sample is a small piece from an automobile fuel tank with a multilayered structure (see Figure 2.1). The properties of the specimen were shown in Table 1.1. The experimental test-bed, in reflection mode, is shown in Figure 6.1.

6.2. Thickness Measurement

The sample is placed on the designed device to band sample to different curvature. The whole device with the sample is immersed in a water tank. A focusing lens is used for our experiments. A transducer, in a normal incidence, works as a transducer-receiver. The ultrasonic pulse propagates through the coupling fluid and reflects on the water / sample interface to produce echo *Sa*. The part of pulse echo *Sb*, transmitted through the sample is totally reflected at second interface the up-HDPE layer and up-glue layer. Echo *Sc* is reflected at third interface that is glue layer with barrier layer. The fourth echo *Sd* is reflected from the fourth interface barrier layer and the second glue layer. The echo *Se* is reflected from the fifth interface, the glue layer and bottom HDPE layer. Echo *Sf* is the last reflected at interface between the bottom HDPE layer and fluid (see Figure 6.2).

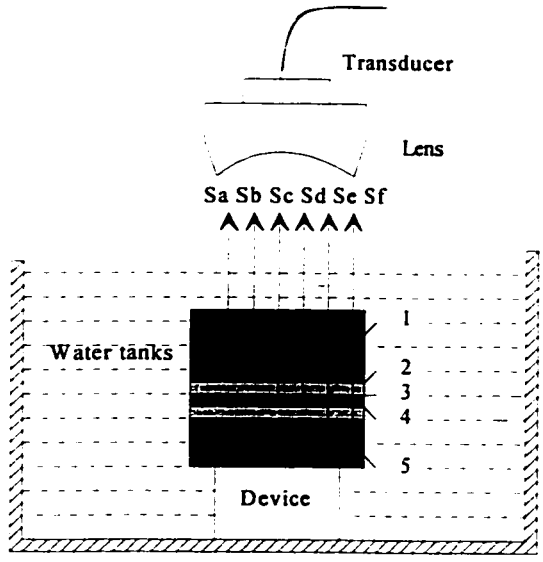

Figure 6.1 The Set-up for Ultrasonic pulse-echo technique
1. The Up-HDPE Layer, 2. The Up-Glue layer, 3. The Barrier Layer
4. The Second Glue Layer, 5. The Bottom HDPE Layer

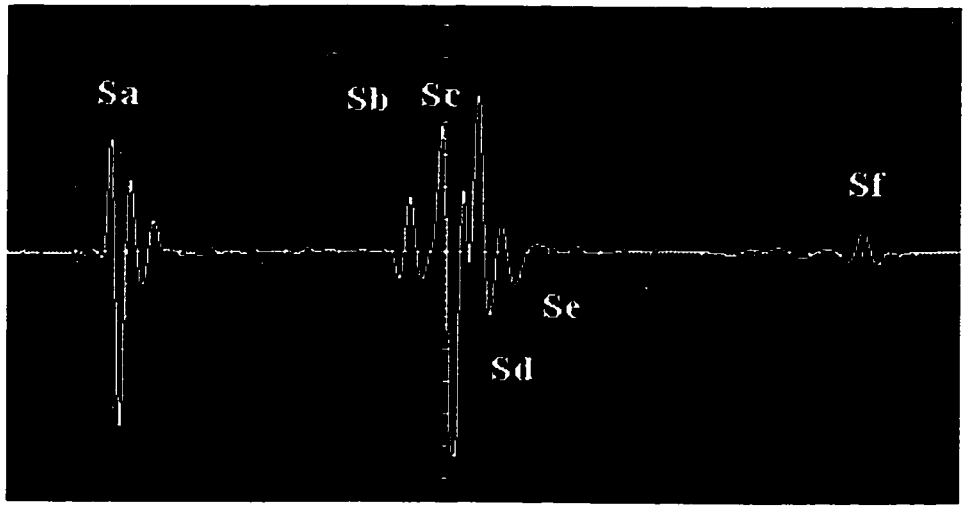

Figure 6.2 Time representation of echoes.
Sa: signal reflected from surface.
Sb: signal reflected from the interface between first thick layer and glue.
Sc: signal reflected from the interface between the glue and barrier.
Sd: signal reflected from the interface between the barrier and glue.
Se: signal reflected from the interface between the glue and bottom thick layer.
Sf: signal reflected from bottom surface.

When we can separate temporally two successive echoes, the measurements of time-delays allow us to calculate sample thickness. Simultaneously, let $\Delta\tau_{ab}$, $\Delta\tau_{bc}$, $\Delta\tau_{cd}$, $\Delta\tau_{de}$ and $\Delta\tau_{ef}$ be respectively the time delay of pulse echo *Sa, Sb, Sc, Sd, Se* and *Sf.* Then, the thickness can be obtained from following expressions: $\Delta\tau_{ab}$

$$
\begin{aligned}
L &= v \times \Delta\tau \\
2L_{HPD1} &= v_{HPDE1} \cdot \Delta\tau_{ab} \\
2L_{AD1} &= v_{AD} \cdot \Delta\tau_{bc} \\
2L_{EVON} &= v_{EVON} \cdot \Delta\tau_{cd} \\
2L_{AD} &= v_{AD} \cdot \Delta\tau_{de} \\
2L_{HPDE2} &= v_{HPDE2} \cdot \Delta\tau_{ef}
\end{aligned}
\qquad \ldots(6.1)
$$

where: v = ultrasonic velocity, $\Delta\tau$ = time between boundary, L = layers thickness

6.3 Results and Discussion

For our experiment we used two transducer frequency/lens focal distance combinations: 15 MHz/ 19 mm and 20 MHz/13 mm. The radius of curvature of the sample were: 30 mm, 36 mm, 50 mm, 60 mm, 80 mm, 85 mm, 93 mm and 134 mm. Generally, when readings of graduated scale are taken, an estimation is made for the final digit — an estimation of the time delay between fine scale graduations, such as 0.01 ns. That could cause thickness calculation with errors range about ± 5 % of the thickness. The numerical values reported as results are the average of ten measurements from optimal focus distance of the acoustic lens taken on the specimen with a given radius of curvature.

The relative errors given in Table 6.1 and Table 6.2, are the estimated average errors from each measurement. Experimental results are shown in Tables 6.1 and 6.2. From Figure 6.3 to Figure 6.7 represent the results of calculation of five different layer's thickness.

Table 6.1. The Experimental Results Using Frequency of 20 MHz

Radius of Curvature R (mm)	HDPE Up Layer ± 0.012 (mm)	Glue Layer 1 ± 0.011 (mm)	Barrier Layer ± 0.016 (mm)	Glue Layer 2 ± 0.011 (mm)	HDPE Bottom Layer ± 0.012 (mm)
30	1.532	0.171	0.387	0.131	2.032
36	1.536	0.173	0.386	0.130	2.027
50	1.543	0.172	0.385	0.131	2.019
60	1.550	0.173	0.387	0.130	2.014
80	1.564	0.173	0.386	0.129	1.998
85	1.580	0.173	0.386	0.129	1.987
93	1.583	0.174	0.385	0.129	1.977
134	1.584	0.174	0.386	0.127	1.974
flat	1.586	0.174	0.387	0.127	1.974

Table 6.2. The Experimental Results Using Frequency of 15 MHz

Radius of Curvature R (mm)	HDPE Up Layer ± 0.012 (mm)	Glue Layer 1 ± 0.011 (mm)	Barrier Layer ± 0.016 (mm)	Glue Layer 2 ± 0.011 (mm)	HDPE Bottom Layer ± 0.012 (mm)
30	1.532	0.172	0.387	0.132	2.027
36	1.543	0.172	0.386	0.131	2.024
50	1.558	0.173	0.387	0.129	2.017
60	1.559	0.173	0.387	0.129	2.013
80	1.562	0.173	0.386	0.129	2.005
85	1.566	0.173	0.386	0.128	1.998
93	1.576	0.173	0.387	0.127	1.986
134	1.577	0.174	0.387	0.127	1.971
flat	1.576	0.174	0.387	0.127	1.972

The "flat" is an expression of test non-curved the sample, the results were the average of ten measurements by using both 15 and 20 MHz frequencies.

In Figure 6.3, the normalized barrier layer thickness is plotted against the radius of the sample's curvature. As seen in this figure, when the sample is flat, both 15 MHz and 20 MHz lenses have the same (0.387 mm) results. When the radius of the curvature of the samples is increasing to 134 mm, the specimen is banded less. The value is very close to the data obtained from measuring on the flat specimen.

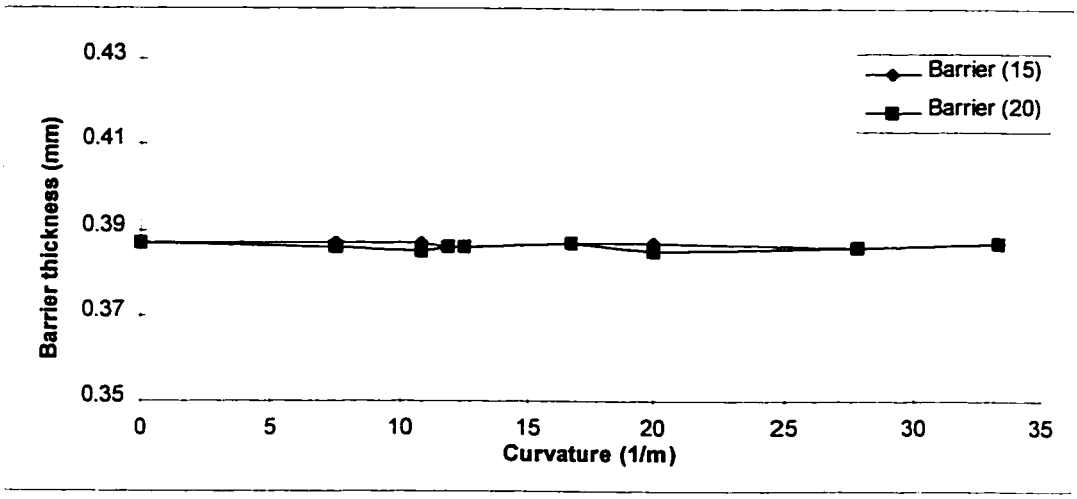

Figure 6.3 The Thickness of Barrier Layer

As seen in Figure 6.4, the top HDPE layer thickness is plotted with the radius of the sample's curvature. Figure 6.4 shows the top HDPE layer thickness is increasing as the radius of sample's curvature is increasing. When the specimen has a small radius of curvature, the specimen has been bent the most and the top layer of the specimen is stretched and thinned. When the radius of curvature of the sample is increased, the top layer is extended less and the thickness is gradually increased close to flat one's thickness.

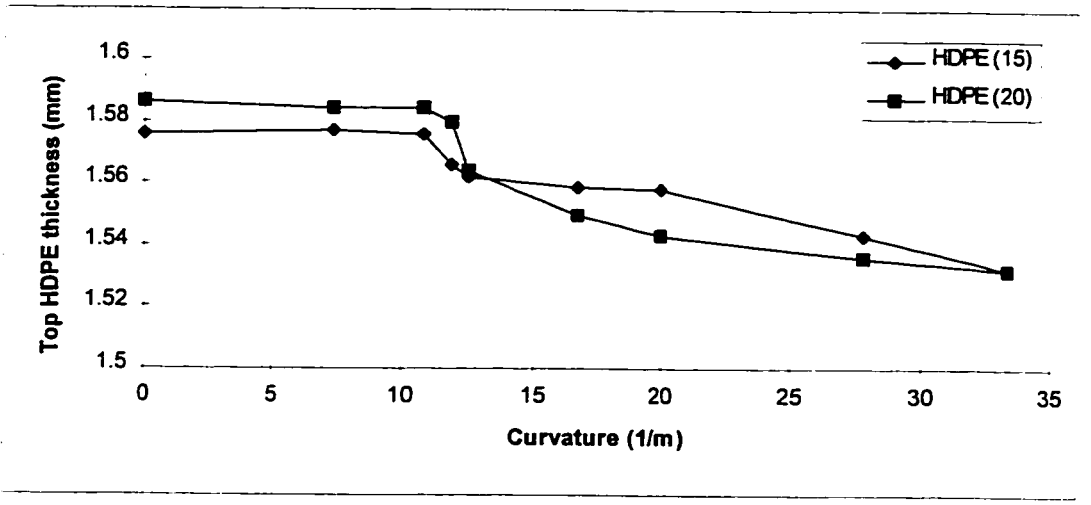

Figure 6.4 The Thickness of Top-HDPE Layer

In Figure 6.5, the top glue layer thickness is plotted against the radius of the sample's curvature. In this figure, when the radius of curvature of the sample is increased, the top layer is extended less and the thickness is gradually increased. When the radii of curvature are 93 mm and 134 mm, the top glue layer thickness is very close to the flat value for both 15 MHz and 20 MHz transducers.

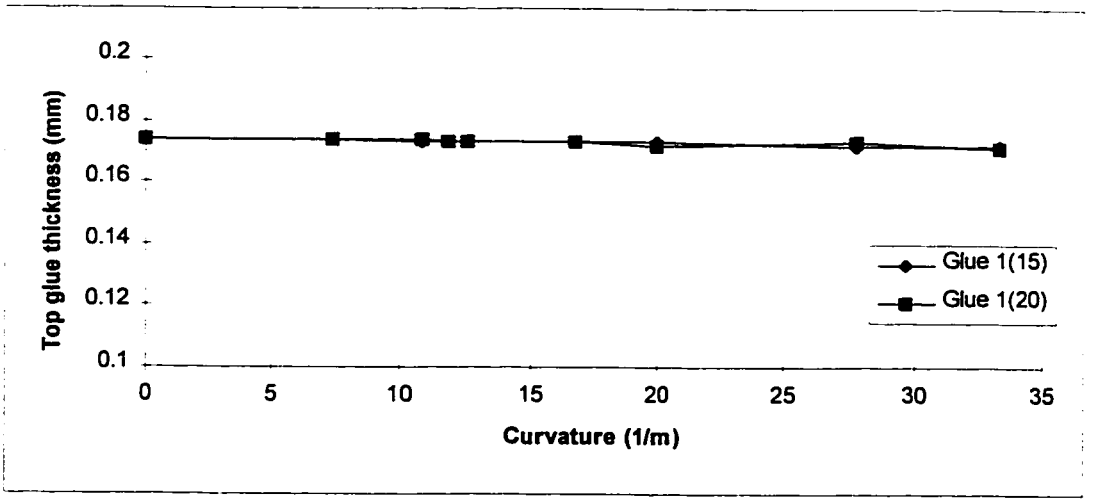

Figure 6.5 The Up Glue Layer Thickness

Figures 6.6 and 6.7 show the bottom glue layer's thickness and bottom HDPE layer's thickness decreases as the radius of sample's curvature increases. These figures clearly show that when the specimen has a small radius of curvature the bottom layer of the specimen is compressed and thickened. When the radius of curvature is increased, the bottom layer is compressed less and the thickness is gradually decreased close to the flat value.

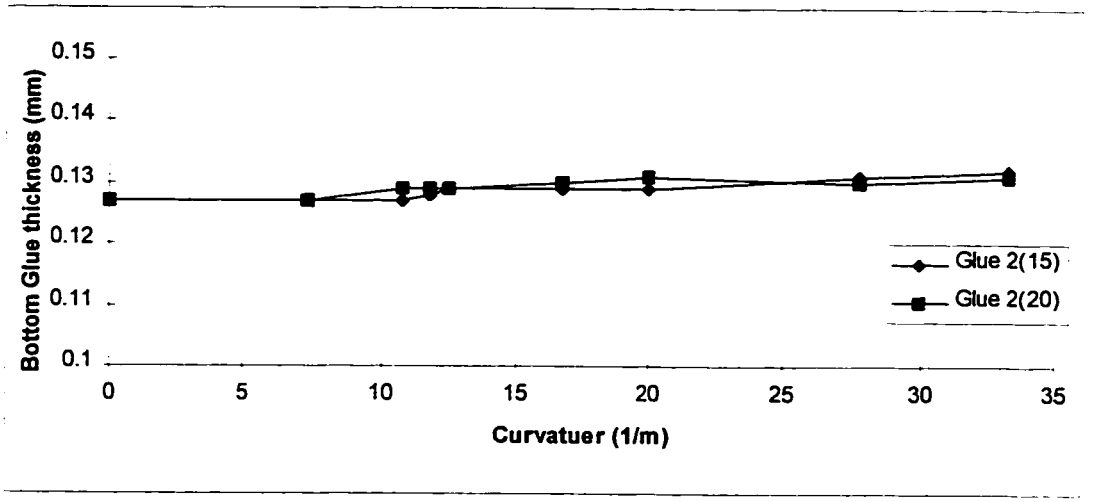

Figure 6.6 The Second Glue Layer Thickness

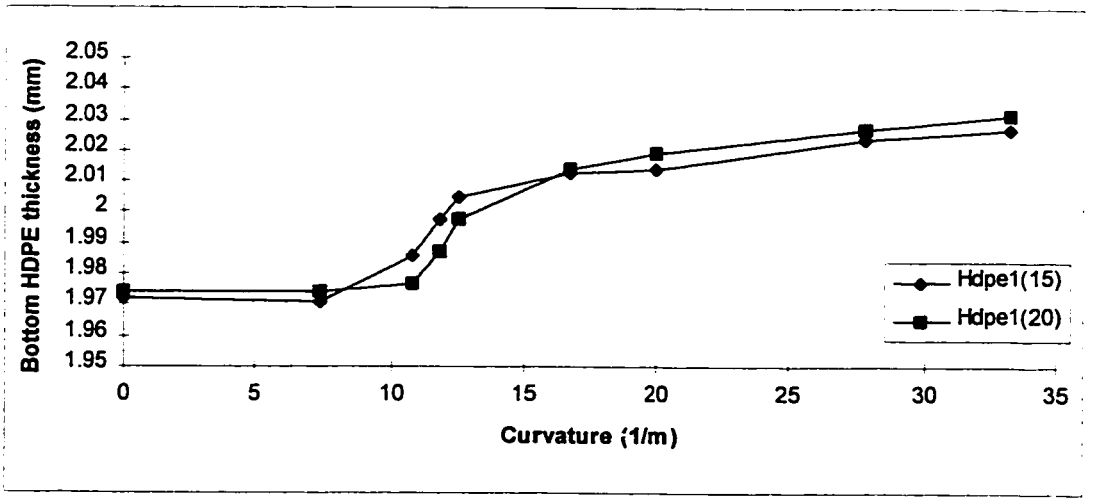

Figure 6.6 The Bottom HDPE Layer Thickness

The result of the ultrasonic pulse-echo measurement system can be affected by many factors including:

(1) Measuring error due to the effect of a sample's geometric characteristic. One of the factors that affects measuring error is the curvature of a sample's surface and the curvature of its internal layer. As the radius of each layer's curvature is different in its curved multilayered system, it will reduce the amplitude of the information (second layer, third layer ...) of the reflected echo signal with respect to the internal layer thickness.

(2) Errors due to the subjectivity of the operator. A certain portion of the measuring error occurs with operating experience in the use of an oscilloscope. There are three potential methods for estimating the peak time delay: (a) measuring the time difference between the peaks in the signal, (b) measuring the time difference between the rising edges of each peak and (c) measuring the time difference between the center of each peak. Some errors might occur in the measurements depending both on the operator's qualifications and his or her working experience.

(3) Errors due to a change in the amplitude and the shape of the bottom echo-signal. When working with ultrasonic thickness measurement the amplitude and shape of the bottom echo signal changes according to the acoustic and geometric characteristics of the

sample being inspected (the attenuation of ultrasonic vibrations in the material, the thickness of the sample, the curvature, the roughness and nonparallelism of the surface).

The signal can also change because of interaction between the bottom echo-signal and signals of acoustic and electrical noises. Those are the main reasons to change the amplitude and shape of the bottom echo signal, which associates the incremental duration of the measurement time interval [35].

Those are three major reasons for errors in the experiment. The Ultrasonic pulse-echo waveform is a very complex waveform, resulting from multiple reflections of different modes of wave propagation. With the advanced technology of signal processing available today, this suggests that a large number of ultrasonic pulse-echo signal parameters can be adjusted during the experiment.

CHAPTER 7

CONCLUSION AND FUTURE STUDIES

The feasibility of using the ultrasonic method based on time-delay of reflected pulse echoes to measure the thickness of individual plies in a curved multilayered structure has been demonstrated. The carried out experimental work of this thesis has shown good agreement between theoretical results and experimental data. The optimization algorithm is used for the determination of the distance between the focus lens and the curved sample surface has been applied for investigation of multialyered structures.

Our experiments also demonstrated sufficient spatial and depth resolution results for quantitative measurement of the individual internal plies in a curved multilayered sample. The comparison of our experimental results with various kinds of lenses demonstrates the advantages for applying focusing lenses to measuring a curved solid, because in this case it is more concentrated on the particular small area, which under inspection and more reflected signals from the material interfaces are received by the transducer/receiver.

The ultrasonic pulse echo technique has been shown to be quite effective in determining the layer thickness of curved multilayered polymer structures despite the weak reflections from the boundaries. This is potentially useful in the manufacturing of automobile fuel tanks, since the thickness could be measured during the process. Ultrasonic testing has already proved to be a valuable tool for nondestructive flaw detection in materials. This tool has the potential for increasing the quality and reliability of plastic fuel tanks and other types of containers. Further work in this promising application may result in sensitivity and accuracy improvements.

REFERENCES

[1] **R.-I. Yu. Kazhis, L. Yu. Mazheika, A. A. Vladishauskas, A. Kh. Vopikin, and V.S. Volkov,** Theoretical and Experimental Study of the Generation of Pulsed Acoustic Field in Objects with Curved and Rough Surface, *Defktoskopia*, No. 1, pp. 73-81, January, 1989.

[2] **P.C. Pedersen, D.P. Orofino**, Modeling of receiving signals from finite reflectors in pulse-echo ultrasound, *Ultrasnoics Symposium*, pp.1177-1181, 1994.

[3] **G. Kossoff, D.A. Carpenter, D.E. Robinson**, A Sonographyic technique to reduce beam distorting by curved interfaces, *Ultrasound in Med. & Biol.* Vol. 15, No. 4, pp. 375-382, 1989.

[4] **Michael J. S. Lowe**, Matrix techniques for Modeling Ultrasonic Waves in Multilayered Media, *IEEE Transaction on ultrasonics, Ferroelectrics and Frequency Control*, Vol.42 No.4, pp. 525-542, July 1995.

[5] **Josef Krautkamer and Herbert Kraurkramer,** *Ultrasonic Testing of Materials*, 1990.

[6] **W.M. Ewing, W.S. Jardetzky**, and F. Press, *Elastic Waves in Layered Media.* New York: McGraw-Hill, 1957.

[7] **I.A. Viktorov**, *Rayleigh and Lamb Waves*. New York :Plenum Press, 1970.

[8] **G.A. Farnell and E.L. Adler**, "Elastic wave propagation in thin layers," in Physics Acoustic,Principles and Methods, W. P. Mason and R.N. Thurston, Ed. New York: Academic Press, 1972, Vol. IX, pp. 35-127, 1972.

[9] **Leonid, M. Brekhovskikh**, *Wave in Layered Media.* New York: Academic Press, 1960.

[10] **L.M. Brekhovskikh and V. Goncharov**, Mechanics of continua and Wave Dynamics. Berlin: Springer-Verlag, 1985.

[11] **W.T. Thormson**, Transmission of elastic wave through a stratified solid medium, *J. Appl. Phys.*, Vol. 21, pp. 89-93, 1950.

[12] **N. A. Haskell**, The Dispersion of Surface Waves on Multilayered Media. *Bulletin of the Seismological Society of America*, p.17-33. 1953.

[13] **T. H. Watson**, A Note On Fast Computation of Rayleigh Wave Dispersion in The Multilayered Elastic Half-Space. *Bulletin of the Seismological Society of America*, Vol. 60, No. 1, pp. 161-166, February, 1970.

[14] **F. A. Firerstone**, *J. Acoust. Soc. Am.* Vol. 18, pp.200, 1946.

[15] **E. A. Hidemann**, Phy. 107, pp. 463-473, 1937.

[16] **S. Sokolov**, Ultrasonic Methods for Investigation of the Properties of Heat Treated Steel and for Detecting Internal Defects in Metallic Objects. *Tech. Phy.* 11, pp. 160-169, 1941.

[17] **T. Kundu, A.K. Mal, R.D. Weglein**, Calculation of the Acoustic Material Signature of a Layered Solid. *J. Acoust. Soc. Am.* 72. p.353-361, February 1985.

[18] **C.C.H. Guyott, P. Cawley**, *J. Acoust. Soc. Am.* 83. February 1988.

[19] **Chantal Martin, Jean-Jacques Meister, Marcel Arditi and Pierre-Andre Farine**, A Novel Holographic Processing of Ultrasonic Echoes for Layer Thickness Measurement. *IEEE Transaction on Signal Processing*, Vol. 40 No. 7, pp. 1819-1825, July 1992.

[20] **Christopher Graciet, Bernard Hosten**, The measurement of through thickness plate vibration using a pulsed ultrasonic transducer. *Ultrasonics Symposium*, pp. 1219-1222, 1994.

[21] **Richard P. Cooker and Richard E. Challis**, *Automatic Algorithms for Digital Signal Processing to Characterize the Propagation of ultrasound in Thin Adhesive Layers.* Ultrasonics International 93 Conference Proceedings, pp. 299-302, 1993.

[22] **Adnan H. Nayfeh and Timothy W. Taylor**, Surface wave characteristics of fluid-loaded multilayered media, *J. Acoust. Soc. Am.* 84(6), pp. 2187-2191, December 1988.

[23] **Jens Kuause and Bernhard Schwierzi**, *Thickness Measurement On Multiilayered Structures By saw Dispersion.* AMD-Vol. 140, Acoustic-Optics and Acoustic Microscope ASME. 1992.

[24] **N. A. Haskell**, The Dispersion of Surface Waves On Multilayered Media, *Bulletin of the Seismological Society of America*, pp. 17-31, 1951.

[25] **R.P. Shaw and P. Bugl**, Transmission of plane waves through layered linear viscoelastic media", *J. Acoust. Soc. Am.*, pp. 649-654, 1968.

[26] **C. T. Sun**, Surface Waves in Layered Media, *Bulletin of the Seismological Society of America*, Vol. 60, No.2, pp. 345-366, April, 1970.

[27] **Diter Scheider**, Thomas Schwarz and Bernd Schultrich, Determination of elastic modulus and thickness of surface layers by ultrasonic surface waves, Thin Solid Films, Vol. 219, pp. 92-102, 1992.

[28] **B. A. Auld**, *Acoustic Fields and Waves in Solids.* volume 1 and 2, Robert E. Krieger Publishing Company, Malabar, Florida, 1990.

[29] **M. Bashyam**, Thickness-compensation technique for ultrasonic evaluation of composite materials, *Material Evaluation*, November, pp. 1360-1364, 1990.

[30] **Otto R. Gericke**, Computer Based Ultrasonic Multiple Frequency Pulse-Echo Test System, *Int. N.D.T.*, Vol. 10, pp. 13-42, 1984.

[31] **R. G. Maev, E. Yu. Maeva**, Imaging of Deep Internal layers in Layered Polymer System Using The Ultra-Short Pulse Acoustic Microscope, *Conf. on Electrical Insulation & Dielectric Phenomena, IEEE Dielectrics and Electrical Insulation Society*, San Francisco, USA, Oct. 20-23, 1996.

[32] **O. R. Gerick**, *J. Acoust. Soc. Am.*, Vol. 36, pp. 313-322, 1964.

[33] **Don E. Bary; Don McBride**, *Non-Destructive Testing Technique,* John Wiley & Sons, Inc., 1990

[34] **A. Briggs**, *Acoustic Microscopy*, Clarendon Press, Oxford, 1992.

[35] **V. A. Kalinin and V. L. Tarasenko**,Measuring-Error Components of Ultrasonic Thickness Gauges Using Two-Element Separate-Combined Piezoelectric Transducers, *Radiative, Optical, and Other Methods*, Plenum Publishing Corporation, pp. 658-666, 1988.

[36] **Frank Longbottom and Halit Eren**, Ultrasonic Multiple-Sensor Solid Level Measurements, *IMTC.*, pp. 749-752, May, 1994.

[37]. **Vikram K. Kinra, Changyi Zhu, Paul Jaminet and Vasu Iyer** , Low-Frequency Ultrasonic NDE of an Interphase Layer, AMD. Vol.177, *Ultrasonic Characterization and Mechanics of Interfaces*, ASME 1993

[38] **Alex Vary**, Ultrasonic Measurement of Materials Properties, *NDT.* v.13, pp. 1-38, 1986.

[39] **James H. Williams, Jr, Samson S. Lee and Hira Karagulle**, Input-Output Characterization of an Ultrasonic Testing Systems By Digital Signal Analysis, *Int. NDT.* V.12 pp. 147-192,1986.

[40] **P.P. Goswami**, Numerical Simulation of Ultrasonic Transmission Through Curved Interface, *International Journal for Numerical Methods in Engineering*, Vol. 36, pp. 2369-2393, 1993.

[41] **Hyung-Chul Chol, John G. Harris**, Scattering of an Ultrasonic Beam from a Curved Interface, *Wave Motion*, 11, p.383-406, 1989.

[42] **Jens Krause**, Thickness Measurement on Multilayered Structure by SAW Dispersion, *Ultrasonics*, Vol. 32, No. 3, pp.195-199, 1994.

[43] **D. L. Folds, C. D. Loggins**, Transmission and Reflection of Ultrasonic Waves in Layered Media, *J. Acoust. Soc. Am.*, Vol. 62, No.5, p. 1102-1109, November, 1977.

[44] **Y. Z. Ruan, L. B. Felsen**, Reflection and Transmission of Beams at a Curved Interface, *Journal of Optical Society of America*, Vol. 3, No. 4, pp.566-579, April 1986.

[45] **Dale Ensminger**, *Ultrasonics Fundamentals, Technology, Applications*, New York: Marcel Dekker, Inc., 1988.

[46] **C. Craciet, B. Hosten**, Simultaneous Measurement of Speed, Attenuation, Thickness and Density with Reflection Ultrasonic Waves in Plate, *IEEE Ultrasonics Symposium*, pp. 1219-1222, 1994.

[47] **Heninich Kuttruff**, *Ultrasonics, Fundamental and Applications*, Elseview Applied Science, London and New York, 1991.

[48] **Peter D. Edmonds**, *Methods of Experimental Physics*: volume 19 Ultrasonics, Academic Press, New York, 1981.

[49] **Mathias Fink**, Time Reversal of Ultrasonic Field-Part I: Basic Principles, *IEEE Transaction on ultrasonics, Ferroelectrics and Frequency Control*, Vol.39, No.5, pp. 555-566, September, 1992.

[50] **Francois Wu, Jean-Louis Thomas, and Mathias Fink**, Time Reversal of Ultrasonic Field-Part II: Experimental Results, *IEEE Transaction on ultrasonics, Ferroelectrics and Frequency Control*, Vol.39, No.5, pp. 567-578, September, 1992.

[51] **Didier Cassereau and Mathias Fink**, Time Reversal of Ultrasonic Field-Part III: Theory of Closed Time-Reversal Cavity, *IEEE Transaction on ultrasonics, Ferroelectrics and Frequency Control*, Vol.39, No.5, pp. 579-592, September, 1992.

[52] **W. J. Surovik, R. J. Gulde, Don E. Bary and K. T. Hartwig**, Shell Thickness Measurements in Composite Conductors Using Ultrasonics, *Nondestructive Evaluation*, Vol. 11, pp. 13-16, 1993.

[53] **Ronald A. Roberta**, Model of the Acoustic Microscopy Response to Scattering by a Near-Surface Void, *J. of Nondestructive Evaluation*, Vol. 9, No. 2/3, pp. 181-196, 1990.

[54] **Henry L. Bertoni**, Ray-Optical Evaluation of V(z) in the Reflection Acoustic Microscopy, *IEEE Transactions on Sonics and Ultrasonics*, Vol. su-31, No.2, March, 1984.

[55]. **R. B. Thompson, D. O. Thompson, D. K. Holger, D. K. Hsu, M. S. Hughes, E. P. Papadakis, M. Tsai, and L. W. Zachary**, Ultrasonic NDE of Thick Composites, *J. Nondestructive Evaluation*, Vol. 10, pp. 43-56, 1991.

[56] **Stephen L. Rosen**, *Fundamental Principles of Polymeric Materials*, John Wiley & Sons, Inc., 1993.

[57] **F. L. Mathews and R. D. Rawlings**, *Composite Materials: Engineering and Science*, Chapman & Hall, 1994.

[58] **Lawrence E. Kinsler, Austin R. Frey, Alan B. Coppens and James V. Sanders**, *Fundamentals of Acoustic*, Third Edition, John Wiley & Sons, 1980.

[59] **Allen Nussbaum and Richard A. Phillips**, *Contemporary Optics for Scientists and Engineers*, Prentice-Hall, Inc., 1976.

[60] **Milles V. Klein**, *Optics*, John Wiley and Sons, Inc. 1970.

[61] **R. S. Longhurst**, *Geometrical and Physical Optics*, John Wiley and Sons, Inc. 1967.

[62] **L. Marton and C. Marton**, *Methods of Experimental Physics: Polymers*, Part C: Physical Properties, Edited by R. A. Fava, Academic Press, 1980.

[63] **G. K. Batchelor**, *Sound Pulses*, Cambridge at University Press, 1958.

[64] **Max Born**, *Principles of Optics*, Fifth Edition, Pergramon Press, 1975.

[65] **Francis A. Jenkins and Harvey E. White**, *Fundamentals of Optics*, Third Edition, McGraw-Hill Book Company, Inc., 1957.

[66] **Warren P. Mason and R. N. Thurson**, *Physical Acoustics*, volume 10, Academic Press, New York, pp.1-126, 1973.

[67] **Paul R. Williamson and M. H. Worthington**, Resolution Limits in Ray to Graphy Due to Wave Behavior: Numerical Experiments, *Geophysics*, vol. 58, No. 5, pp. 727-735, May, 1993.

[68] **Jonathan M. Rubin, Ronald S. Adler, J. Brian Fowlkes and Paul L. Carson**, Phase Cancellation: A cause of Acoustical Shadowing at the Edges of Curved Surfaces in B-Mode Ultrasound Images, *Ultrasound in Med. & Biol.*, Vol. 17, No. 1, pp. 85-95, 1991.

[69] **Todd M. Trimble, Smaine Zeroug, D. E. Chimenti and L. B. Felsen**, *Acoustic Beam Reflection From Cylindrical Fluid-Loaded Elastic Structures*, Ultrasonics International 93 Conference Proceedings, pp. 755-758, 1993.

[70] **Hyung-Chul Choi and John G. Harris**, *Focusing of An Ultrasonic Beam by a Concave Interface*, Elastic Waves and Ultrasonic Nondestructive Evaluation, Edited by S. K. Datta, Elsevier Science Publish, B.V. (North-Holland), pp. 177-182, 1990.

[71] **Carl K. Frederickson and Philip L. Marston**, Travel Time Surface of a Transverse Cusp Caustic Produced by Reflection of Acoustic Transients From a Curved Metal Surface in Water, *J. Acoust. Soc. Am.*, pp. 650-659, February, 1994.

[72] **C. J. Randall and Fred E. Stanke**, Mathematical Model for Internal Ultrasonic Inspection of Cylindrical Layered Structures, *J. Acoust. Soc. Am.*, pp. 1295-1305, April, 1988.

[73] **Catherine Potel and Jean-Francois de Belleval**, Surface Wave in an Anisotropic Periodically Multilayered Medium: Influence of the Absorption, *J. Appl. Phys.* 77 (12), pp. 6152-6161, 15, June, 1995.

[74] **Jacques Arman and Said Akker**, *Characterization of the Interface Between Two Polymers by Surface Acoustic Waves*, Ultrasonics International 93 Conference Proceedings, pp. 269-272, 1993.

[75] **Yosif Golfman**, Ultrasonic Non-Destructive Method to Determine Modulus of Elasticity of Turbine Blades, *Sample Journal*, Vol. 29, No. 4, pp. 31-35, July/August 1993.

[76] **Carl K. Frederickson and Philip L. Marston**, Transverse Cusp Diffraction Catastrophes Produced by the Reflection of Ultrasonic Tone Bursts From a Curved Surface in Water: Observations, *J. Acoust. Soc. Am.*, pp. 2869-2877, November 1992.

[77] **S. Ya Gmyrin**, Effect of Contact Surface Roughness on The Indications of Ultrasonic Thickness Gauges, *Defektoskopiya*, No. 10, 29-43, pp. 189-210, 1993.

[78] **C. M. Langton, A. V. Ali, C. M. Riggs, G. P. Evans and W. Bonfield**, A Contact Method for The Assessment of Ultrasonic Velocity and Broadband Attenuation in Cortical and Cancellous Bone, *Clin. Phys. Meas.*, Vol. 11, No. pp. 243-249, 1990.

[79] **H. Lydia Deng**, Acoustic-Wave Propagation in Thin-Layered Media with Steep Reflectors, *Geophysics*, Vol. 59, No. 10, pp. 1593-1640, 1994.

[80] **P. P. Goswami and T. J. Rudolphi**, Numerical Simulation of Ultrasonic Transmission Through Curved Interface, *International Journal for Numerical Method in Engineering,* Vol. 36, pp. 2369-2393, 1993.

[81] **G. Kossoff, D. A. Carpnter, D. E. Robinson, D. Ostry and P. L. Ho**, A Sonographic Technique to Reduce Beam Distortion by Curved Interfaces, *Ultrasound in Med. & Biol.*, Vol. 15, No. 4, pp. 375-382, 1989.

[82] **H. Kanai, T. Kimura and N. Chubachi**, Accurate Determination of Transit Time of Ultrasound in Thin Layers, *Electronics Letters* , Vol. 31, No. 13, pp. 1109-1112, June, 1995.

[83] **Alain Berry and G. A. Daigle**, Controlled Experiments of The Diffraction of Sound By A Curved Surface, *J. Acoust. Soc. Am.* 83 (6), pp. 2047-2058, 1988.

[84] **Wolfgang Saches, A. G. Every and I. Grabec**, Quantitative Ultrasonic Measurements In Composite Materials, *Nondestructive Evaluation*, Vol. 10, pp. 77-88, 1991.

[85] **V. K. Kinra and C. Zhu**, Frequency-Domain Ultrasonic NDE of Three-Layered Media: The Inverse Problem, *Journal of De Physique,* IV, pp. C5-1151-1160, 1994.

[86] **Yusuke Tsukahara, Noritaka Nakaso, Jun-Ichi Kushibiki and Noriyoshi Chubachi**, Excitation of Plate Waves in Thickness Measurements of Layers Deposited on Thin Plates, *IEEE Transaction on Ultrasonics, Ferroelectrics and Frequency Control*, Vol. 36, No. 6., pp. 638-642, 1989.

VITA AUCTORIS

NAME:	Hong Shao
PLACE OF BIRTH:	Shanghai, P.R.China
YEAR OF BIRTH	1963
EDUCATION	Shanghai Maritime University, Shanghai, P.R. China.
	1982-1986 B.Sc.
	University of Ottawa, Ottawa, Ontario, Canada
	1994-1995
	University of Windsor, Windsor, Ontario, Canada
	1995-1997 M.A.Sc.

IMAGE EVALUATION
TEST TARGET (QA-3)

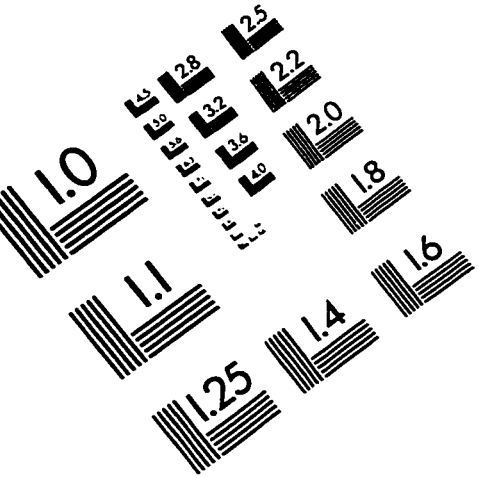

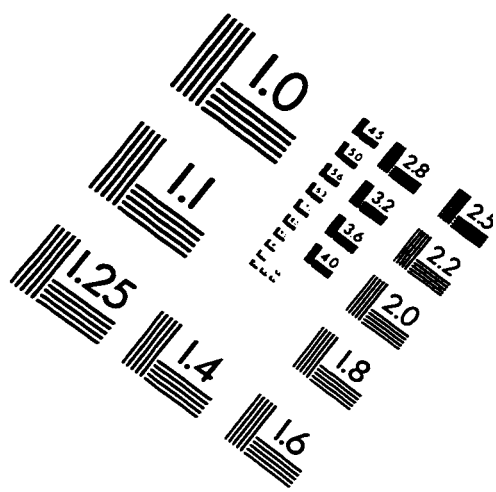

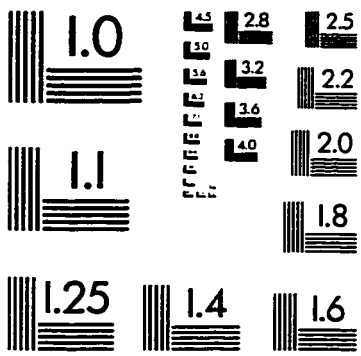

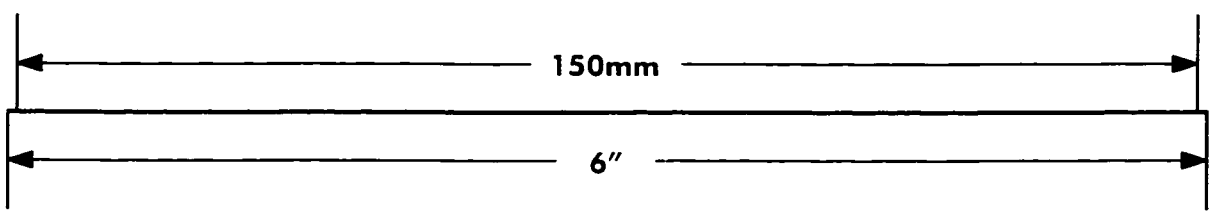

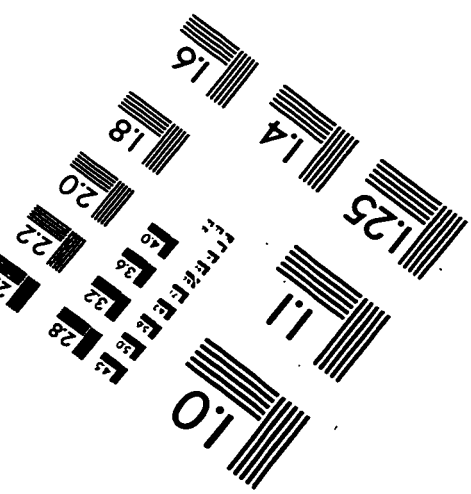

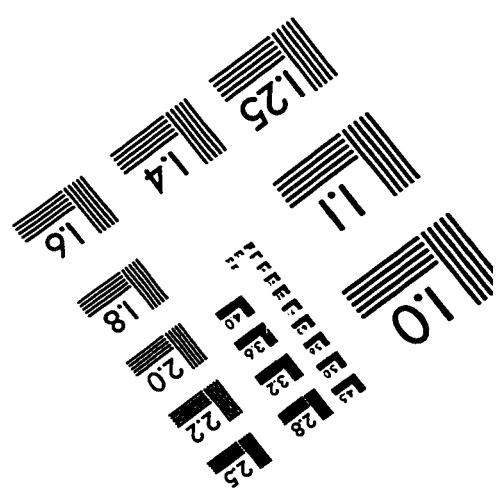

APPLIED IMAGE, Inc
1653 East Main Street
Rochester, NY 14609 USA
Phone: 716/482-0300
Fax: 716/288-5989